NBSIR 84-2895

Modeling of Smoldering Combustion Propagation

U.S. DEPARTMENT OF COMMERCE
National Bureau of Standards
National Engineering Laboratory
Center for Fire Research
Gaithersburg, MD 20899

June 1984

U.S. DEPARTMENT OF COMMERCE

NATIONAL BUREAU OF STANDARDS

MODELING OF SMOLDERING
COMBUSTION PROPAGATION

T. J. Ohlemiller

U.S. DEPARTMENT OF COMMERCE
National Bureau of Standards
National Engineering Laboratory
Center for Fire Research
Gaithersburg, MD 20899

June 1984

TABLE OF CONTENTS

LIST OF TABLES

LIST OF FIGURES

MODELING OF SMOLDERING COMBUSTION PROPAGATION

T. J. Ohlemiller

Introduction

Smoldering combustion is defined here as a self-sustaining, propagating exothermic reaction wave deriving its principal heat from heterogeneous oxidation of the fuel (direct attack of oxygen on the fuel surface). The primary context for considering this type of process here is fire safety. Such processes also occur in other contexts such as cigarette smolder or underground coal gasification; results from these areas will be discussed to a limited extent where pertinent.

Smoldering, like flaming, is a combustion process which spreads through a fuel when heat released by oxidation is transferred to adjacent elements of the fuel. While spread of smoldering and flaming both occur through coupled heat release and heat transfer mechanisms, smoldering typically yields less complete oxidation of the fuel, lower temperatures and much slower propagation rates. However, all of these smolder characteristics can vary widely with oxygen supply. Stable smoldering is possible in some circumstances at air/fuel ratios only a few percent of stoichiometric[*]. At the opposite extreme, a strong oxygen supply can raise the intensity and temperature of smolder to such a degree that gas phase reactions become dominant and flaming propagation takes over.

---

[*]Air/fuel ratio as used here refers to the ratio of the fluxes of air and fuel entering the reaction zone (as seen by an observer moving with the reaction zone).

1

Fire safety hazards involving smoldering. Only rather recently has

smoldering been recognized as a major fire safety hazard in the United States.

Clarke and Ottoson (1) found cigarette ignition of bedding and upholstery

materials to be the single largest cause of residential fire deaths. The

cigarette, itself a smoldering cellulosic fuel, is nearly ideal as a smolder

initiator in susceptible fabric and filling materials. In such materials, a

self-sustaining smolder process can often be established well before the

cigarette is consumed. This particular problem is coupled to both fabric and

filling response to heating (2, 3, 4, 5). Once established in this manner,

smoldering becomes a steadily growing generator of carbon monoxide and other

toxic gases as the size of the reacting region enlarges. This smoldering

process may spread stably for an hour or so then abruptly transition to

flaming combustion. The hazard in this context (and others) is thus two

fold - toxic gases during smoldering and rapid destruction following flaming

transition. Which of these is most responsible for the observed death toll is

not fully clear; there has been some analysis of this question which impli-

cates both smoldering and subsequent flaming (6).

The increasing interest in residential energy conservation has resulted

in a strong demand for effective insulating materials, particularly for attics

where heat losses are greatest. Cellulosic loose-fill insulation is quite

effective and comparatively inexpensive. It is essentially ground wood, being

made mainly from recycled newsprint, reground to a fibrous, fluffy form that

is blown into place. The oxidation chemistry of wood clearly renders this

material combustible. A variety of additives, typically in fine powder form,

are included in an effort to control this combustiblity. They are rather

effective in supresing flaming but are less so for smoldering. When the

2

insulation is improperly installed, heat sources such a recessed light fixtures can cause smolder initiation (7, 8, 9, 10). Once started, this smolder becomes self-sustaining, spreading through an attic space and posing the same toxicity and flaming-potential hazards as in the above case.

The two problem areas above, upholstery/bedding and cellulosic insulation smoldering, have received the most attention; they are also the most extensively studied in some respects. (It should be noted that the former problem is by far the more common, probably because of much more frequent encounters with the ignition source, i.e., a cigarette.) There are numerous other problems, however. For example, wood and certain other low permeability building materials (particleboard sheathing and some types of rigid foam insulation) can smolder, especially in configurations where surface heat losses are suppressed (11, 12, 13). Spontaneous heating and ignition, usually to smoldering combustion, have long been a problem with a variety of natural products, usually cellulosic in nature (14, 15). In industries which process oxidizable materials in finely divided form there is a danger not only from dust explosions (a flaming problem) but also from smoldering ignition of dust layers accumulating within or on top of the hot processing equipment (16). A significant fraction of grain elevator fires, for example, begins with smoldering (17).

Some experimental characteristics of smolder propagation. Table I is brief summary of the smolder behavior observed for a variety of fuels in several configurations. The list of results is by no means complete but it gives a representative picture of smolder in organic materials. The study by Palmer (11) presents the most complete parametric examination of smolder

3

behavior for configurations that are rather complex but realistic. The study by Ohlemiller and Lucca (18) is the first systematic comparison of configurations simple enough to be modeled in detail. (The forward/reverse terminology is explained below.)

Cellulosic materials show up most frequently in Table I because they are so common and nearly all of them smolder. There are, of course, numerous other materials with the potential to smolder but both the material and the way it is used must be favorable to smoldering in order for it to emerge as a fire safety hazard. Note that all the materials listed are fibrous or particulate and thus tend to have a rather large surface to volume ratio; they also comprise a fuel mass permeable to gas flow and diffusion. The current discussion will ultimately focus on fuels in such a physical form.

The various results in Table I generally support the description of smoldering as a slow, low temperature combustion phenomenon that responds with increased vigor when the oxygen supply is enhanced. The slowness is apparent in the magnitude of the smolder velocities. It is interesting to note that these do not vary greatly (except for a cigarette during a draw) in spite of wide variations in fuel type and configuration. This probably reflects an oxygen-supply-rate-limited character of the process; a process limited by the fuel oxidation kinetics would be expected to vary more with various materials. The low temperatures generally reflect the fact that smoldering causes quite incomplete oxidation of the carbon and hydrogen in the fuel. Part of this incompleteness is probably a consequence of the detailed nature of the surface reactions but part is also a result of how various configurations minimize or preclude gas phase oxidation of surface-derived molecules (pyrolytic or oxidative).

Figure 1 gives a detailed view of the structure of a smolder wave in a fairly typical configuration, i.e., a horizontal fuel layer smoldering by natural convection/diffusion in ambient air. The fuel is a permeable, low density layer of wood fibers. The details of these results are discussed more fully in Ref. 24 but several features are noteworthy. The thickness of the fuel layer decreases quite substantially as a result of smoldering. The wave structure is very much multi-dimensional. Heat losses (e.g., from the top surface) have a substantial impact on the thermal structure. It is inferred in Ref. 24 that the overall shape is probably largely determined by oxygen diffusion and that two successive overall stages of heat release are coupled together to drive the propagation process. It is apparent that realistic smolder problems can be quite complex. The work of Baker on the structure of the reaction wave in a smoldering cigarette elaborates upon this considerable complexity (25-28); this body of work provides more details on the structure of this rather unique smolder problem than can be found for any other problem of this nature.

Plan of this paper. The smolder initiation problem has been quite extensively studied at least from a thermophysical point of view (29, 30). Propagation subsequent to ignition is considerably more complex and much less studied. In the present work, questions pertaining to ignition are not examined. Transition from smoldering to flaming is not examined in any detail due to the current, almost total lack of information on the nature of this process. The focus here is on the coupled processes of chemical heat generation and heat transfer involved in sustained smolder propagation. This review begins with an overview of the types of chemical processes involved. The nature of both the heat sources and the heat sinks is examined; it will be

5

apparent that even for cellulose, the most extensively studied fuel, detailed chemical mechanisms are lacking. Next a rather general model of the propagation process is posed in order to provide a complete picture of all the interacting phenomena, both chemical and physical, that may play a role. This model is more comprehensive than any previously posed in the literature though it is limited to situations described by a continuum solid/gas hypothesis. The model is not solved, rather it serves as a benchmark for assessing the simplifications present in the models thus far solved in the literature. The general model is re-cast in dimensionless form to permit inferences about the sizes of parameter groupings which justify simplications. Finally, the smolder models in the literature are examined in light of these considerations; the existing models will be seen to fall well short of adequately describing realistic smolder propagation problems such as that in Figure 1.

Chemistry of Smoldering Combustion

In very general terms, smoldering involves the exothermic attack of heat and oxygen on condensed phase polymeric materials at a rate sufficient to overcome heat losses and thus be self-sustaining. In the absence of oxygen, the typical polymeric fuel will be endothermically degraded by heat to smaller volatile molecules, sometimes also leaving a solid residue of a variable aromatic nature referred to as a char; this char pyrolyzes much more slowly than the initial polymer*. The participation of sufficient oxygen in this process results in its having a net exothermicity. The heat could arise from one or more of three sources:

---

*There is some confusion in the literature over the use of the term"char". Here the term refers to the black solid residue which typically remains after the end of the initial rapid weight loss upon heating of a polymer. Pyrolytic gasification of this char is usually much slower than that of the initial polymer.

6

(1) oxygen participation in the polymer degradation process,

(2) oxygen attack on the volatilized molecules produced by
     the degradation, or

(3) oxygen attack on the char residue.

The extent of the contribution to smoldering from each of these potential
sources (with the exception of some aspects of (3)) is not very well
quantified for any fuel (and, of course, it will vary with the chemical nature
of the fuel and, possibly with the conditions of heating of a given fuel). To
model smolder propagation, one needs rate expressions for all significant heat
release processes and competing heat sink processes.

In examining these potential sources in greater detail, frequent
reference to results for cellulose will be made; it is the most-studied
smolder-prone polymer.

Gas Phase Oxidation. It is assumed, from indirect evidence, that gas
phase oxidation of volatilized molecules does not provide the majority of the
exothermicity which drives smolder propagation. Flames, per se, are usually
not visible during smoldering. Most frequently used retardant chemicals that
act as flame suppressors are not of much use in stopping smoldering (3, 31).
(There are some chemicals that suppress both flaming and smoldering, at least
in some tests (32)). Finally, smoldering is most frequently encountered in
fuels with a large surface to volume ratio which would encourage solid surface

attack of oxygen and tend to suppress gas phase radical chain reactions through surface quenching of the free radicals (33, 34). While this argues against a dominant role for gas phase oxidation, it does not preclude a significant supplementary role.

Any supplemental contribution from gas phase oxidation reactions can be expected to increase as the peak smolder temperature increases (and as the surface to volume ratio of the fuel decreases). Baker presents evidence for significant gas phase oxidation (on a time scale of $\sim$ 10s) of H_2 and CO produced from tobacco in the temperature range 500-900°C (35). Extrapolation of Dryer's (36) kinetics for homogeneous oxidation of "wet" CO indicates that CO can be oxidized on a time scale of seconds at 600°C. Propane, fairly representative of many hydrocarbon molecules, can be oxidized even below 400°C on a time scale of ten seconds (34). However, all of these cases except the cigarette involve experimental conditions where the radical chain reactions in the gas would not be suppressed by the proximity of a large amount of solid surface.

Gas phase heat release contributions from the oxidation of other more complex molecules arising from the polymer degradation process will be highly dependent on their chemical nature (and thus, in turn on the nature of the original polymer). This has received little attention in the context of smoldering and more work is needed. Open tube flow reactor studies of the overall oxidation rate of specific polymer gasification products would presumably yield only the upper limit on the potential reaction rate during smoldering; the suppressing effect of a large amount of solid surface areas would be missing. Packed tube studies would be more pertinent but the

8

surface/volume ratio and the nature of the surface would become additional variables. For example, the oxidation of propane, mentioned above, is suppressed up to 550°C in the presence of an extended surface of glass (34).

It is interesting to note that, in contrast to the inferred secondary role of gas reactions in smoldering, in one configuration of in situ coal combustion (reverse combustion, defined below), the sole heat source is taken to be gas phase oxidation of vaporized fuel molecules (37, 38).

It appears likely that the many smoldering processes whose peak temperature is well below 600°C receive only supplemental heat input from gas phase reactions, if any. On the other hand, the usual view that smoldering is driven mainly by analogs of the classic graphite oxidation reactions when oxygen attacks the char may be too simple. It ignores the possible exotherm from oxygen attack on the original polymer or partially degraded versions of it; it also glosses over the complexity of the char itself which is not pure carbon.

Oxidative Polymer Degradation. Look next at the question of exothermicity from oxidative degradation of the polymer. Nearly all polymers, thermosetting or thermoplastic, are subject to exothermic oxygen attack if the temperature is sufficiently high; such processes have been extensively studied, though mainly at temperatures and heating rates lower than in smoldering (39). Thermoplastic polymers will normally contract under surface tension forces when heated, minimizing their surface area and causing endo-thermic pyrolysis to dominate; smoldering is thus precluded. However, if the thermoplastic polymer is coated on a rigid support with extended surface area

9

that does not decrease with temperature (e.g., pipe lagging), a considerable exotherm can result, sometimes causing smoldering ignition (40). Char-forming polymers that initially have a large surface-to-volume ratio tend to retain it during degradation; exothermic oxidative degradation, if favored chemically, thus can continue in parallel with char-forming reactions (the two may be coupled in some polymers). In all types of polymer these oxidative reactions tend to compete with purely pyrolytic reactions which are usually endothermic. Given this competition between oxidative and pyrolytic degradation, the net outcome in terms of exo- or endothermicity depends on the chemical nature of the polymer and the circumstances of the heating (heating rate, ambient oxygen concentration, surface-to-volume ratio). Thus, in attempting to assess the importance of oxidative degradation of a polymer as a heat source in smolder propagation, one must focus on a specific situation. Unfortunately, it is very difficult to learn many details of the smolder chemistry by studying the propagation process itself.

Thermoanalytical techniques (thermogravimetry (TG) and differential scanning calorimetry (DSC)) provide a controlled environment (fixed oxygen level, linearly programmed heating at 1-10°C/min) that can yield at least an engineering characterization of smolder chemistry. These techniques have been applied to various materials in a high specific surface area form including cellulose fibers (41, 42), lignin powder (42), wood fibers (44), polyurethane, polyisocyanurate and phenolic foams (13) and tobacco powder (45, 46). One finds a qualitatively similar result, for heating in air, in all cases. The DSC thermogram, which provides a measure of heat production or absorption of the sample during heating, typically shows <u>two</u> major exothermic peaks. The first peak begins just as the sample starts to degrade rapidly and lose

10

weight. The second corresponds to oxidation of the char residue left by the first stage of degradation. Given these facts alone, it would be reasonable to identify the first peak with oxidative pyrolysis of the original polymer or its immediate condensed phase degradation products (the first heat source listed above).

Shafizadeh and Bradbury (47) investigated this question of oxidative pyrolysis in more detail for pure cellulose. It was shown that during prolonged isothermal heating in air at 190°C, oxygen attack on cellulose is indeed substantial, leading to a build-up and ultimately a steady-state concentration of hydroperoxide groups and greatly accelerated production of CO and CO_2. However, it was found that for isothermal heating at temperatures above 300°C, weight loss in air is no faster than in pure nitrogen implying that, by this temperatue, the oxidative pyrolytic reactions are overwhelmed by the purely thermal pyrolytic reactions. On the other hand, Shafizadeh, et al. (41) found, upon comparing linearly programmed heating (15°C/min) of cellulose in nitrogen and in air, that the presence of oxygen substantially enhances the rate of cellulose gasification up to 350°C where DSC results show the first exotherm to be peaking. In ref. 41 the first exotherm is attributed to chemisorption of oxygen on the condensed phase material (presumably radicals) formed during pyrolysis, not to oxidative attack on the original cellulose molecules. The chemisorption hypothesis appears to have derived from studies of the considerable exothermicity evolved when O_2 is adsorbed on cellulosic chars; however, these chars were formed at substantially higher temperatures, 400-500°C (45). Most recently, Shafizadeh and Sekiguchi (43) presented further evidence derived from nuclear magnetic resonance and infrared studies of the condensed phase. The solids examined were residues left from

isothermal (325-600°C) and programmed heating (10°K/min) of cellulose. An apparent qualitative correlation between the amount of aliphatic carbons in the residue and the size of the first exotherm measured from this residue by DSC in air, lead to the conclusion that the source of this first exotherm is oxidative attack on these aliphatic carbons. For residues created by first heating cellulose in nitrogen at 400°C, the proposed heat source seems quite convincing. For cellulose exposed directly to air during heating, the evidence is less convincing; it is this latter situation that is most pertinent to cellulose smoldering. The overall work of Shafizadeh and co-workers is strongly suggestive of a pyrolytically-initiated, oxygen-altered exothermic degradation process contributing to cellulose smolder but its exact nature is not clear at present.

A significant secondary result of the study by Shafizadeh and Sekiguchi (43) was a demonstration that the heat measured during DSC experiments with cellulose residues in air is proportional to the quantity of non-pyrolyzable solid and not to the amount of pyrolysis vapors generated. This supports the widely-used assumption that the DSC is measuring the heat of heterogeneous oxidation and not gas phase heat from oxygen attack on evolved fuel-like molecules.

The impetus for defining the nature of the first exotherm seen in DSC thermograms of cellulosic materials lies in its dominant role during smolder initiation (9, 10) and its substantial contribution to smolder propagation (18, 24). It is likely that the first exotherm seen with the other materials mentioned above can play a similarly significant role in their smolder characteristics. Thus the available evidence points to the likelihood of a

12

significant role for oxidative pyrolysis as an appreciable heat source in many smoldering processes.

Char Oxidation. The solid residue left at the end of the first DSC exotherm (defined here as char) is typically a predominantly carbonaceous material with a substantially enhanced surface area due to pore formation (23, 48). The important role of this char in many smoldering processes is not in dispute; its oxidation is highly exothermic (heat source number (3) listed above). The heat release from this source can be dominant in some configurations; however, it can be less critical or even absent in others. The crucial factor is oxygen access to the various stages in the fuel degradation process, as will be discussed below. Polymer chars are not unique chemical entities but rather depend on the thermal history of formation; with continued heating they change further (49, 50). The mechanism of emergence of a pore system, which for some starting materials is totally absent, has not received any scrutiny in the context of smoldering in spite of its obvious pertinence to surface oxidation. Much more is known about this subject for coals where the existing pore system evolves during gasification (51, 52); models of the coal pore system and its evolution have been developed (53, 54).

Low temperature cellulosic chars (typical of smoldering) are much more readily attacked by oxygen than is pure carbon. Shafizadeh and Bradbury hypothesize, however, that the oxidation of the char proceeds by a mechanism similar to that proposed elsewhere for carbon (55, 56). The proposed oxidation mechanism of carbon begins with oxygen chemisorption at a surface free radical site. The surface complex falls into one of two broad classes. The first class of complexes is quite stable and dissociates only at very high

13

temperatures (up to 1000°C). The second class is mobile and reactive, quickly forming both CO and CO_2 which then desorb from the surface. These mechanistic proposals have not yet been fully confirmed or quantified.

The formation, reactivity and oxidation products of cellulosic chars are greatly influenced by the presence of inorganic additives or impurities. Alkali metals such as sodium, calcium and magnesium have a strong influence on the ability of cellulosic materials to smolder (12, 57). This complicates modeling efforts in as much as kinetic rate constants found in the literature for the oxidation of a cellulosic char are unlikely to hold for cellulose obtained from some other source. Shafizadeh has shown that small amounts of inorganic materials such as sodium chloride or boric acid can alter the rate of heat release from a cellulose char by at least a factor of two up or down (relative to a char from pure cellulose) depending on the additive (58); the effect is achieved in large measure through changes in the product ratio CO/CO_2 from the surface oxidation of the char but significant kinetic effects may also exist (41).

Other reactions can gasify a carbonaceous char. Thus CO_2, H_2O and H_2 (which may arise from pyrolytic or oxidative reactions) can remove carbon from the solid in the form of CO or CH_4. These reactions are believed to be less important in many smolder problems. Attack by the first two of these gases is endothermic; the third is exothermic. Available data indicate that they will proceed at a significant rate only above 650-700°C (52) even in the presence of catalytic impurities (59). Many smolder processes proceed stably at substantially lower temperatures. The peak temperature is largely dependent on the rate of oxygen supply, however, so, as with gas phase oxidation

14

reactions, the relevance of these is dependent on the smolder conditions of interest. Cigarette smolder is one problem in which both the diffusive oxygen supply and the forced flow oxygen supply are normally sufficient to keep the peak temperature above 850°C; Baker (35) has shown that CO_2 reduction on tobacco char is significant in this case. In the most common mode of <u>in situ</u> coal gasification (forward mode, defined below), these non-oxidative gasification reactions are of central importance since they account for the bulk of the coal char conversion to gases (60).

Substantial Heat Sinks : Pyrolysis and Water Vaporization. It was noted above that endothermic pyrolysis of the polymeric fuel competes with exothermic oxidative degradation. The endothermicity of the pyrolytic reactions is comparatively small on a unit mass basis but it can be an important heat sink during smoldering, nevertheless, since a large fraction of the fuel may undergo this process. These reactions are again specific to the polymer of interest. Pyrolytic degradation of polymers has been extensively examined (39, 61). Such degradation typically proceeds by free radical chain reactions in the condensed phase involving a complex interplay of chain initiation, propagation, transfer and termination reactions. For complex polymers such as cellulose, the monomeric unit may come apart in further parallel reactions resulting in a large variety of volatile products. If the polymer forms a pyrolytic char, aromatic condensation reactions building a cross-linked char must be progressing in parallel with the other reactions. Despite this complexity, full details of which are rarely available, the net process of weight loss can frequently be described by relatively simple expressions. Bradbury, et al (62), showed, for example, that pyrolytic weight loss from cellulose can be empirically described by a three reaction model.

15

Water constitutes a significant fraction of some organic fuels, particularly the smolder-prone cellulosic materials. It is also a major product of oxidation. Movement of this water in and out of the condensed phase by condensation and evaporation can provide a substantial local heat effect and can also alter the overall rate of smolder propagation. The specific effects can depend significantly on whether the water, once vaporized, is carried into higher temperature regions thus remaining a vapor, or is carried into a region where it will recondense. The rate of evaporation or condensation is frequently taken to be mass transfer limited (by the boundary layer external to the fuel particle) with the particle phase water vapor pressure assumed to be in equilibrium with the particle temperature. This last assumption may well fail when the particle water content is low (63); empirical correlations may prove necessary (64).

Simplified Kinetic Model. The degree of detailed description of the above chemical processes necessary in modeling smolder propagation depends on the purpose of the model. In fire research, one is seeking to understand first the controlling factors in the propagation process with the ultimate goal of learning how to prevent it. In a first cut at this, it is usually sufficient to insert into the model some reasonably accurate description of the major chemical heat effects; this calls for "global kinetics" in which real chemical species other than oxygen are not described. The drawback of this approach is that it offers no clues about how changes in chemical mechanisms might be exploited to suppress smoldering. If the goal were to model the toxicity of smoldering, one would have to incorporate the generation/consumption reactions of the major toxicants (usually CO); such a goal can rapidly lead to increased model complexity. Some goals mandate
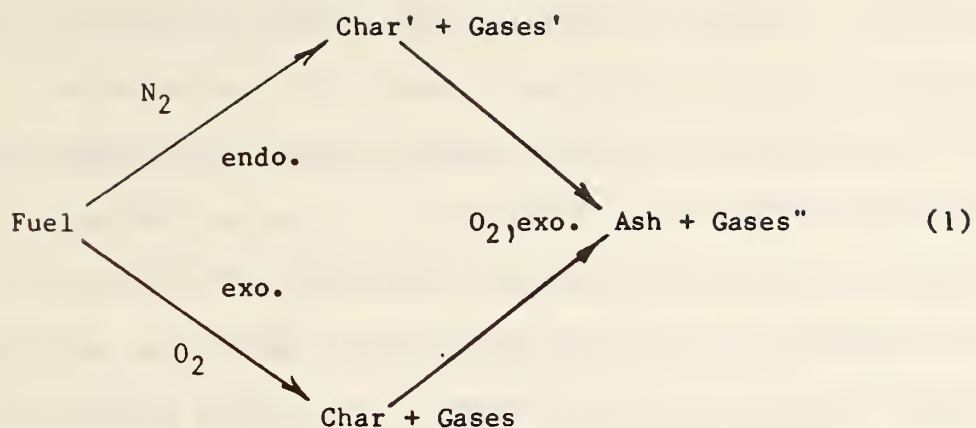
16

seemingly intractable complexity. Modeling of cigarette smolder with the goal of learning to control the numerous flavor-related or health-related species is such a problem (65). However, if the species of ultimate interest are present in minor amounts, so as not to have a signficant impact on the smolder wave structure when they are created or destroyed, the problem can be uncoupled. The wave structure can be solved using "global kinetics" only; the history of the minor species can then be tracked as they ride through this pre-determined wave structure (45).

In any event, it should be apparent from the preceding discussion, that even for cellulose, the full mechanistic details of the smolder chemistry, much less the quantified rate expressions, are not available. Inevitably then, one must resort to substantial simplifications in modeling smolder chemistry.

It was noted above that thermal analysis techniques are of some use in characterizing the "global kinetics" of gasification and the heat effects accompanying it. The results must always be utilized with caution since the heating rates during smolder ($0(10^1$ to 10^3 °C/min)) can sometimes greatly exceed the useable heating rates in thermal analysis ($\leq 0(10^1$ °C/min)). Such differences in heating rate could potentially alter the controlling chemical and/or physical processes. Higher heating rates cause the peak rate of any elemental reaction to shift to higher temperatures where the reaction then proceeds faster. The limiting step in a given heterogeneous oxidation reaction could shift at higher temperatures from chemical control (adsorption, surface reaction or desorption) to physical control (oxygen diffusion). Furthermore, competing parallel reactions with differing activation energies

17

will be shifted upward in temperature differing amounts (less with increasing activation energy); this could shift the controlling mechanisms in a complex elemental reaction sequence. In spite of this caveat, these techniques are frequently used; available higher heating rate techniques suffer from considerable experimental inconvenience (66, 67). It is somewhat comforting that the extrapolation in heating rates from thermal analysis to smolder is less than with nearly any other combustion process; nevertheless it poses unanswered questions.

There are available in the literature a wide variety of techniques for fitting kinetic expressions to thermogravimetry data (68, 69). These can be used to obtain the "global kinetics" of gasification and heat generation/consumption; typically, techniques employing multiple heating rates give kinetic parameters most suited to extrapolation. This has been done for a polyurethane (70), tobacco (45) and wood fibers (44). Since, as noted above, the thermal analysis results for these materials yield only two global reaction peaks in the presence of oxygen and one in the absence of oxygen, one can obtain a reasonably adequate picture of the "global kinetics" of the fuel gasification by fitting the following scheme to the thermal analysis behavior (44).

$$\text{Char' + Gases'}$$

$$\text{Fuel} \quad \overset{N_2}{\underset{\text{endo.}}{\nearrow}} \quad \overset{\text{exo.}}{\underset{O_2}{\searrow}} \quad O_2, \text{exo.} \quad \text{Ash + Gases''} \qquad (1)$$

$$\text{Char + Gases}$$

This scheme has the principal qualitative features of smolder chemistry discussed above. An endothermic pyrolytic path competes for the original fuel with an exothermic oxidative degradation path. Both paths form a char which is subject to exothermic oxidation. Gas phase oxidation of the product gases is not included in the thermal analysis scheme. Thermogravimetry will not see such processes, of course. Furthermore, one can infer from the short gas residence time in a DSC sample holder ($< 1s$) and available data on oxidation of such species as CO or H_2 (likely products as a typical char is gasified around 400-500°C) that the DSC will measure only the heterogenous heat effects (36, 71). (This may not be the case with inhibited chars that gasify at higher temperatures but recall that Shafizadeh and Sekiguchi (43), as noted earlier, provided experimental evidence that the DSC is measuring only heterogeneous reaction heat for cellulose.) If gas phase chemical heat effects are to be included in a smolder model, they must be quantified by some other means.

This reaction scheme leaves much to be desired as a description of smoldering combustion chemistry. Even as a pragmatic device for approximate description of chemical heat effects during smoldering, its use must be

examined case by case. Recall, for example, that Bradbury, et al (62) required a three step reaction scheme just to empirically describe the pyrolytic gasification of cellulose whereas Eqn. (1) would assign only one step to this process. In this case, Bradbury, et al required the extra complexity in part to describe the temperature-dependent variability in quantity of char formed during cellulose degradation. Failure to include this effect could yield misleading results in a model of cellulose smolder applied over a broad range of conditions. Note also that Eqn. (1) does not directly fit the most recent mechanistic ideas proposed by Shafizadeh and Sekiguchi (43) for the first exotherm from cellulose, i.e., that is caused not by immediate cellulose oxidation but rather by oxidation of a condensed phase cellulose degradation product. On the other hand, Eqn. (1) has been used to give a reasonable description of a related material, wood fibers (44).

In summary, modeling of smolder propagation requires empirical rate expressions for the major heat sources and heat sinks. If the peak smolder temperatures do not exceed 600°C, the major heat effects are probably attributable to oxidative polymer degradation, char oxidation, polymer pyrolysis and water movement. Thermal analysis techniques can provide empirical rate and heat effect data on the first three of these but these data must be utilized with caution to model the higher heating rate processes during smoldering. A considerable amount of information on the details of the chemistry involved in smoldering combustion of even such a common material as cellulose is still lacking; this precludes construction of smolder models with anything more than a global representation of the fuel chemistry.

A General Model of Smolder Propagation in a Fuel Bed

Thermophysical Considerations. Although the degradation and oxidation
chemistry of the fuel is quite complex, it is only one side of the smolder
propagation problem. The rate of oxidation of the char, for example, can
depend not only on the intrinsic chemical processes occurring at active sites
on the char surface but also on the specific surface area available for
reaction (m^2/g of char), the local temperature and the local oxygen concentra-
tion. The local oxygen concentration depends in turn on the rate at which it
can reach the reaction neighborhood. Typically, in fire-safety related
smolder problems, the oxygen originates in the ambient atmosphere and must
penetrate the permeable bed of fuel by buoyant flow and diffusion. As seen
from Table 1, the fuel bed frequently consists of a large array of fuel
particles[*]; their flow permeability is typically much less than that of the
fuel bed itself. Pores may exist or develop in the fuel particles during
degradation allowing oxygen to diffuse inward against a net outward movement
of gasification products. If the pore system is evolving as a consequence of
degradation and oxidation reactions, the surface area available for the oxida-
tion reactions is also changing; a pore system can quickly yield an internal
area for oxidative reactions that is much greater than the external geometric
surface of the fuel particle. The familiar zone concepts for single particle
gasification are then pertinent (72, 75, 52). Zone I is the limiting case in

---

[*]The term particle is used in a very broad sense here. An open cell polymer
foam, for example, actually consists of a continuous solid phase permeated by
a continuous gas phase. We identify the particles in such a case as the
intersecting segments of polymer (generally cylindrical) that frame the
contiguous gas bubbles, mentally isolating a typical intersection as the
center of a typical particle. Solid wood presents a similar but more complex
(and anisotropic) structure; a particle in this structure would be the long,
thin, flat double cell wall that subdivides the gas space.

21

which oxidation reactions (or other gasification reactions) on the internal surface of the particle are very slow compared to the rate of oxygen diffusion inward through the pore system; the oxygen concentration throughout the particle interior is thus virtually uniform. Zone III is the opposite limiting case in which the rate of oxidation in the particle interior is so fast that oxygen cannot penetrate and oxidative reactions are confined to the external surface. Zone II is the more general case in which the oxygen supply and consumption rates in the particle interior are comparable, leading to a non-uniform oxygen concentration. In certain circumstances there may be temperature gradients within the particles as well. In the present smolder problem, there is the further complication that the oxygen concentration and gas temperature around the exterior of individual fuel particles is varying as the overall smolder wave moves through the array of fuel particles (see Fig. 2). Transport of heat and oxygen to the outer surface of fuel particles and through the particle array become additional rate processes that must be considered in determining the overall movement of the smolder reaction front. The model must account for all of these processes which interact with the smolder chemistry.

Similar types of interactions between physical and chemical processes occur in other combustion problems involving coal beds and incinerators as well as in a variety of industrial processes. A systematic development of solutions to simpler and more tractable versions of such problems is the subject of Ref. (73). Analytical solutions to a wide variety of single particle and multiple particle problems are presented.

In describing the following model equations, a major simplification is imposed. The smolder wave is assumed to extend over many fuel particles so that it can be treated as a continuum. Without this assumption, it is necessary to treat each fuel particle and the gas around it separately as it interacts with the gas and all other individual fuel particles; such a model becomes highly specialized to the particular geometric arrangement of particles and their shapes. By making this continuum wave assumption, it is no longer possible to treat such problems as the smoldering of a stack of several logs in a fireplace or wood stove, for example. However, all of the problems noted in Table I are amenable to the continuum assumption. Even the spread of smolder over a single piece of solid wood is treatable if it is viewed as a very low permeability fuel bed of small particles as defined in the preceding footnote (the anisotropy of the wood would have to be carefully accounted for, however).

In formulating a continuum model of smolder wave propagation through a large array of fuel particles, conservation equations are required for the gas phase and the particle phase. Since the fuel bed interacts with its surroundings, a set of boundary conditions is also required to define that interaction. In some cases, such as that in Fig. 1, it is probable that a complete description of the full propagation problem requires a model of the behavior of the surrounding gas coupled to that of the fuel bed. This complete problem has never been addressed. Here it is assumed that some approximate boundary conditions (described below) suffice to isolate the fuel bed alone as the system to be studied.

Recall that the goal here is a rather complete formulation of a model not for the purposes of solution but as an explicit exposition of all the interacting elements in the general problem of smolder propagation. The relative simplicity of existing models in the literature will then be apparent.

Single Particle Equations. Consider first a situation in which gradients in species concentration and temperature exist within the individual fuel particles (Fig. 2) . As will be seen, species gradients are much more likely than temperature gradients in view of the continuum assumption. In contrast to the gradients in the particle phase, the gas phase around each particle is assumed to be locally homogeneous due to rapid molecular and/or turbulent mixing on the scale of a particle; this is a usual assumption in packed bed problems. There still may exist concentration or temperature differences between the locally homogeneous gas phase and the fuel particle surface across a boundary layer. Transport across this boundary layer is treated by the usual packed bed heat and mass transfer correlations (70).

Because of the gradients within the particles, it becomes necessary to formulate conservation equations for the interior of a typical particle. Then, at each locus along the continuum smolder wave it is necessary to account for the interaction between this typical particle and the surrounding gas at that locus within the fuel bed. Note that since the particles may be porous, both gas and solid exist within the particle boundary as well. At any locus within the particle it is assumed that gas and solid are in thermal equilibrium because of the typically very small dimensions of the pores (small fraction of particle radius). The general problem of heat and mass transfer within a single particle is three-dimensional. It is reduced here to one

space dimension with the assumption that the particles approximate a sphere, a cylinder or a thin flat plate. Furthermore, it is assumed that the fuel particles are all initially the same size; a few comments will be added below on the effects of a broad distribution of sizes. The particles are also assumed to be rigid structures. They may lose mass by attrition from the outer surface or from the internal pore surface but they do not go through a plastic state that would allow various forces to deform them; this is a reasonable approximation for most fuels of interest but it could be an over-simplification for some flexible polyurethane foams, for example.

With these assumptions, the following conservation equations apply to the interior of a typical fuel particle. See the Nomenclature table for an explanation of the symbols used.

Conservation of gas mass within particle pores:

$$\frac{\partial}{\partial t} \left(\phi_P \rho_{GP} \right) + \frac{1}{r^a} \frac{\partial}{\partial r} \left(r^a \rho_{GP} v_{GP} \phi_P \right) = \sum_\ell \left(A_{VP\ell} v_{G\ell} R_{P\ell} \right) \tag{2}$$

The first term accounts for transient accumulation of gas within the particle pores, the second term for flow of gas out through the pores (three possible particle geometries depending on value of a); the third term is a summation over the reactions which gasify the particle. As noted above, these comprise both surface oxidation reactions and volumetric pyrolysis reactions. If the particles are completely non-porous, however, the surface reaction term belongs only in the boundary condition at the particle periphery. (Note that pyrolysis will immediately generate pores in a non-porous, non-fluid particle; they will persist unless the particle passes through a subsequent fluid

25

state.) The pyrolytic reactions implicit in the third term do not have a surface area dependence so $A_{VP\ell}$ drops out of those rate expressions.

Conservation of solid mass within particle:

$$\frac{\partial}{\partial t} \left[(1-\phi_P) \rho_P \right] = -\sum_{\ell} \left(A_{VP\ell} \; \nu_{G\ell} \; R_{P\ell} \right) \tag{3}$$

The first term is the transient loss of solid as a net result of the chemical reactions described by the second term; there is no convective term since the particles are rigid.

Momentum of gas in particle pores:

$$\phi_P \rho_{GP} \frac{\partial v_{GP}}{\partial t} + \rho_{GP} \phi_P v_{GP} \frac{\partial v_{GP}}{\partial r} + \phi_P \frac{\partial P_P}{\partial r} = -a_{PD} \mu_{GP} v_{GP} - v_{GP} \sum_{\ell} \left(A_{VP\ell} \nu_{G\ell} R_{P\ell} \right) \tag{4}$$

Here the first two terms account for acceleration of the gas in the pores, the third for the pressure gradient driving the gas flow, the fourth for the drag due to the pore walls (assumed laminar). The fifth term accounts for the acceleration of the gas generated by the various reactions; it appears here because the gas continuity equation has been substituted into the equation.

Conservation of typical gas species in particle pores:

$$\phi_P \rho_{GP} \frac{\partial Y_{jGP}}{\partial t} + \rho_{GP} \phi_P v_{GP} \frac{\partial Y_{jGP}}{\partial r} - \frac{1}{r^a} \frac{\partial}{\partial r} \left(r^a \rho_{GP} D_{ep} \frac{\partial Y_{jGP}}{\partial r} \right)$$

$$= \sum_{\ell} \left(A_{VP\ell} \; R_{P\ell} \; [(\nu_F - \nu_C)_{\ell j} - Y_{jGP} \nu_{G\ell}] \right) \tag{5}$$

26

The gas continuity equation (Eqn. (2)) has been substituted here as well. The first term is due to accumulation of species j in the pores, the second term to convection of the species in the pores, the third to diffusion in the pores. The first part of the reaction term accounts for creation or destruction of species j by any or all of the ℓ reactions in the particle. The second part of the reaction term accounts for dilution by gasification products and comes from substitution of the gas continuity equation. Note that the diffusivity D_{ep} is taken to be the same for all species and it is the effective value in the pores; this can be much less than the free gas value when the pores are comparable to the mean free path of the gas molecules (500-1000 Å pores at 1 atm.) (76). It has been assumed here that there are no gas phase reactions in the pores affecting the species since residence times are generally short and temperatures low (recall the earlier discussion of gas phase reactions on the smolder wave scale); this could require modification in some cases. Oxygen is the gas species of foremost interest.

Conservation of typical condensed phase species in particle:

$$(1 - \phi_P)\rho_P \frac{\partial Y_{jP}}{\partial t} = -\sum_{\ell} \left(A_{VP\ell} \, R_{P\ell} \, [(\nu_F - \nu_C)_{\ell j} - Y_{jP} \, \nu_{G\ell}] \right) \qquad (6)$$

Here Eqn. (3) has been substituted generating the second part of the reaction rate term. Again there is no convective term because the solid is assumed to be rigid.

27

Conservation of gas and solid energy in particle:

$$(1 - \phi_P)\rho_P \frac{\partial h_P}{\partial t} + \phi_P \rho_{GP} \frac{\partial h_{GP}}{\partial t} + \phi_P \rho_{GP} v_{GP} \frac{\partial h_{GP}}{\partial r} - \frac{1}{r^a} \frac{\partial}{\partial r} \left(r^a \lambda_P \frac{\partial T_P}{\partial r} \right)$$

$$- \frac{1}{r^a} \frac{\partial}{\partial r} \left(\sum_{GP} \left(h_{jGP} \rho_{GP} D_{ep} r^a \frac{\partial Y_{jGP}}{\partial r} \right) \right) = \sum_{\ell} \left(A_{VP\ell} R_{P\ell} \left[Q_{\ell,STP} + \right. \right.$$

$$\left. \left. (h_{SP} - h_{GP}) v_{G\ell} \right] \right) \tag{7}$$

Here Eqns. (2), (3), (4), (5) and (6) have been substituted in the original energy balance to obtain the form shown. The first and second terms are due to transient accumulation of sensible enthalpy in the solid and gas, respectively. The third term is due to the enthalpy of the gas convecting in the pores. The fourth term is due to composite gas/solid conduction of heat. The fifth term describes the net diffusion of sensible enthalpy with gases in the pores. The first part of the reaction term is the chemical heat effect (at standard conditions); the second part is a dilution term arising from sensible enthalpy differences between the solid and gas phases. Note that all kinetic energy, pressure work and drag work terms are neglected. Radiation transfer within the particle is also neglected.

Several auxiliary relationships are needed to complement the preceding equations. Each reaction rate (or global reaction) must be explicitly described in terms of temperature and species dependencies. The temperature and species dependence of the transport and thermal properties is required. The perfect gas law is typically assumed to relate gas density, pressure and temperature. The pore system in the particles can be expected to evolve considerably as the various reactions proceed. The mass loss dependence

28

of ϕ_P and $A_{VP\ell}$ could be obtained empirically although little work has been done; most measurements pertain to coal chars (52). There have been a number of attempts to model the evolution of pore systems during gasification of single coal char particles; these are reviewed in Ref. 52. The pore size distribution also affects the effective pore diffusivity D_{ep} and the flow drag constant a_{PD}; a model or empirical data are again necessary.

The two most pertinent boundary conditions on the external particle surface are those for a typical species and for energy transport.

Species:

$$\phi_P \rho_{GP} v_{GP} Y_{jGP} - \rho_{GP} \phi_P D_{ep} \left(\frac{\partial Y_{jGP}}{\partial r}\right)_{r_P} = K \left(Y_{jGP} - Y_{jG}\right) + \left(1 - \phi_P\right) \sum_{\ell} \left(\nu_{G\ell} R_{P\ell}\right) \qquad (8)$$

Here the first term describes convection of the species from the pore system below the particle surface. The second term describes net diffusion of the species to or from the pore system. The third term describes net diffusive plus bulk flow (from particle interior) mass transfer through the boundary layer around the particle. The lumping together of flow and diffusion in one term is conventional if not strictly correct; one must be careful that mass conservation and stoichiometric requirements are satisfied. The fourth term is the source or sink of the particular species due to all reactions on unit area of the exterior surface of the particle.

Energy:

$$\lambda_P \left(\frac{\partial T_P}{\partial r}\right)_{r_P} + H \left(T_P - T_G\right) = \left(1 - \phi_P\right) \sum_{\ell} \left(R_{P\ell} Q_{\ell,T}\right) + \phi_P \rho_{GP} v_{GP} h_{GP} \qquad (9)$$

The first term accounts for composite gas/solid heat conduction in the particle at its exterior surface. The second term describes convective heat transfer across the boundary layer around the particle; it includes conducted heat and sensible enthalpy in products from the particle interior. The third term gives the net source or sink of heat due to reactions on the exterior surface of the particle; note that the reaction heat here is the value at the actual surface temperature. The fourth term is the sensible enthalpy carried by gases emerging from particle pores.

Inspection of Fig. 2 leads one to conclude that this approach to describing the particles with internal gradients cannot adequately describe two modes of energy transfer on the scale of the smolder reaction wave. These are solid-solid conduction and solid-solid radiative transfer. The gradients in the particles are assumed here to be one-dimensional (normal to the exterior surface) whereas the existence of these two transport processes implies an asymmetric temperature distribution in each particle (three-dimensional).

As will be seen, the gas phase around the particles is always treated here as a continuum on the smolder reaction wave scale. In this case, one could approximate the wave-scale heat conduction process as a gas/solid composite process appearing in the gas phase energy equation only; this could even include a radiation-corrected conductivity. The radiation might be better treated by taking the wave-scale distribution of particle surface temperatures (e.g., bottom of Fig. 2) and using it in a radiative transfer model such as the four-flux approximation for a two-dimensional smolder wave (77).

Bulk Solid Equations. If the internal temperature and species gradients (normal to the particle exterior surface) are sufficiently small so that reaction rates within the particle are everywhere the same (Zone I behavior), then it is unnecessary to consider these gradients. The necessary conditions for this will be examined below. If these gradients can be neglected, there is no need to consider individual particles; the condensed phase can be treated as a continuum on the smolder reaction wave scale with no particle scale gradients of interest.

In the equations below, one new physical phenomenon is introduced, that of shrinkage of the fuel bed as it is gasified. It was noted in connection with Fig. 1 that this can be a quite significant effect with some fuels. It is a result of shrinkage of individual particles and possibly deformation of the particles, especially in the case of fibers. A complete description of this phenomenon would require a set of mechanical force balance equations for the fuel bed, coupled together with the conservation equations given below. Rather than do this, an approximation is considered which could be adequate in some cases. Only the possiblility of coherent motions of the bed particles is considered; situations in which individual particles break loose from their neighbors and move several particle diameters under the influence of a force such as gravity are not considered.

The bulk fuel phase equations presented here were derived with a two-dimensional smolder wave in mind; it appears that a third space dimension would not add any new complexity. The coordinate system is fixed in space.

Since the fuel bed can shrink, a differential equation describing the void volume in the bed is needed.

$$\frac{\partial \phi}{\partial t} - \bar{\nabla} \cdot \left[\bar{v}_P (1 - \phi)\right] = n_P \dot{\Lambda}_P \tag{10}$$

This indicates that the transient change in void volume is due to any net flow of particle volume in/out of the control volume and to loss of particle volume upon fuel gasification. Here Λ_P is the flow displacement volume of each particle. It is assumed here that this volume can be empirically measured as a function of mass loss from a particle (e.g., by displacement of a non-wetting liquid such as mercury). Then Λ_P is proportional to the rate of mass loss from the particle.

The particle velocity vector $\bar{v}_P$ in Eqn. (10) is a result of fuel bed shrinkage upon gasification. In a situation such as that shown in Fig. 1, shrinkage downward is probably the most important effect but there is horizontal shrinkage as well with a net particle movement toward the direction of smolder propagation. At least for some fuels, bulk shrinkage of the fuel can be empirically characterized to a first approximation by simply measuring the mass loss dependency of the bulk volume of a fuel bed small enough to be heated uniformly. Given this function, one can estimate the components of $\bar{v}_P$ during smolder propagation with the following:

$$v_{Py} = \int_o^y \frac{d}{dt} \left[V_B(m/m_o)\right]^{1/3} dy' \;\; ; \;\; v_{Px} = \int_x^\ell \frac{d}{dt} \left[V_B(m/m_o)\right]^{1/3} dx' \tag{11}$$

Here $V_B (m/m_o)$ is the empirical, mass-loss dependent, fractional bulk volume function, assumed isotropic. Its rate of change integrated over a path in the

horizontal (x) or vertical (y) direction from the point of interest to an "anchor" point gives the velocity components of the movement of that point. The "anchor" point in the y-direction is the bottom of the layer; in the x-direction, it is the unburned end of the fuel bed. This approach to describing bed shrinkage is clearly approximate; it ignores mechanical aspects of the fuel bed that could hinder the computed movements. At some point during shrinkage, real fuel beds frequently develop cracks because the particles are not free to move. If the cracks are large on the scale of the smolder reaction wave, they may preclude the continuum approach used here.

Conservation of gas in the bulk condensed phase:

$$\frac{\partial}{\partial t}\left[(1 - \phi)\phi_P \rho_{GP}\right] + \bar{\nabla} \cdot \left[\bar{v}_P(1 - \phi)\phi_P \rho_{GP}\right] = (1 - \phi) \sum_\ell \left(A_{VP\ell} v_{G\ell} R_{P\ell}\right)$$

$$- K \ A_{VB} \sum_{KG} \left(Y_{KGP} - Y_{KG}\right) \qquad (12)$$

This is the gas within the pores of the particles. It convects through the fuel bed control volume only as a result of the shrinkage-induced movement of the particles (second term). The gasification reactions in the particles may produce this gas (third term); this is the same set of reactions as in Eqns. (2)-(7). The net transport of gas out of the particles and into the bulk free volume of the fuel bed has both diffusive and bulkflow components. Here it is described in a single lumped mass transfer term (fourth term) as is usual practice for packed bed mass transfer.

Conservation of solid in the bulk condensed phase:

$$\frac{\partial}{\partial t} \left[(1-\phi)(1-\phi_P)\rho_P \right] + \bar{\nabla} \cdot \left[\bar{v}_P (1-\phi)(1-\phi_P)\rho_P \right] = - (1-\phi) \sum_{\ell} \left(A_{VP\ell} \nu_{G\ell} R_{P\ell} \right) \qquad (13)$$

This is basically similar to Eq. (12) except that no solid moves across the particle boundary.

Conservation of typical gas species in bulk condensed phase:

$$(1-\phi)\phi_P \rho_{GP} \frac{\partial Y_{jGP}}{\partial t} + (1-\phi)\phi_P \rho_{GP} \bar{v}_P \cdot \bar{\nabla} Y_{jGP} = (1-\phi) \sum_{\ell} \left(A_{VP\ell} R_{P\ell} \left[\left(\nu_F - \nu_C \right)_{\ell j} \right. \right.$$

$$\left. \left. - Y_{jGP} \nu_{G\ell} \right] \right) - K A_{VB} \left[\left(Y_{jGP} - Y_{jG} \right) - Y_{jGP} \sum_{KG} \left(Y_{KGP} - Y_{KG} \right) \right] \qquad (14)$$

This is a typical gaseous species within the pores of the particles; oxygen is again the species of foremost interest. The gas continuity equation has been substituted in this equation producing the dilution terms that appear as the second part of the reaction and mass transfer terms. Note that any smolder-wave-scale diffusion of these gas species appears not here but in the bulk gas phase species equations.

Conservation of typical solid species in the bulk condensed phase:

$$\left(1 - \phi_P \right)\rho_P \frac{\partial Y_{jP}}{\partial t} + \left(1 - \phi_P \right)\rho_P \bar{v}_P \cdot \bar{\nabla} Y_{jP} = \sum_{\ell} \left(A_{VP\ell} R_{P\ell} \left[\left(\nu_F - \nu_C \right)_{\ell j} + Y_{jP} \nu_{G\ell} \right] \right) \qquad (15)$$

The bulk solid continuity equation (Eq. (13)) has been substituted here producing a result similar to Eq. (14) except for the mass transfer term.

34

Conservation of gas/solid energy in bulk condensed phase:

$$(1 - \phi) \left\{ \phi_P \rho_{GP} \frac{\partial h_{GP}}{\partial t} + (1 - \phi_P)\rho_P \frac{\partial h_P}{\partial t} + \phi_P \rho_{GP} \bar{v}_P \cdot \bar{\nabla} h_{GP} + (1 - \phi_P)\rho_P \bar{v}_P \cdot \bar{\nabla} h_P \right\}$$

$$- \bar{\nabla} \cdot \left[(1 - \phi)\lambda_B \bar{\nabla} T_P \right] + \bar{\nabla} \cdot \bar{S} = H A_{VB}(T_G - T_P)$$

$$+ (h_G - h_P)(1 - \phi) \sum_{\ell} (A_{VP\ell} \nu_{G\ell} R_{P\ell}) + K A_{VB_{KG}} \sum (Y_{KGP} - Y_{KG})(h_{GP} - h_{GK})$$

$$+ (1 - \phi) \sum_{\ell} (A_{VP\ell} R_{P\ell} Q_{\ell,STP}) \tag{16}$$

Eqns. (13)-(15) have been substituted in the original energy conservation
statement for the fuel bed control volume to obtain the form above. As in the
energy equation for a single particle, kinetic energy, pressure and drag work
terms have been neglected. The first four terms (brackets) describe enthalpy
accumulation and convection for both the gas and solid in the bulk condensed
phase. The fuel bed now has a well-defined thermal conductivity although the
condensed phase contribution to it (fifth term) may not be so easily separated
from the gas phase contribution as is done here. Radiative transfer (sixth
term) requires a model such as the four flux approximation mentioned above.
Scattering could appreciably alter radiative transfer in some fuel beds of
interest and, of course, the changing chemical nature of the solid during
smoldering will substantially alter its radiative properties (generally making
the solid more absorbing and less scattering as it is converted to a char).
The seventh term describes convective heat transfer between the bulk solid and
bulk gas phases. The next two terms describe dilution of enthalpy upon solids
gasificaton due to a difference in the specific enthalpy of gas and solid
phases. The last term gives the net rate of chemical heat release due to the
various reactions in the bulk condensed phase.

As with the single particle equations, various auxiliary relationships are needed to complement the above conservation relations. Among those not mentioned in that previous context or in the preceding discussion is the specific area of the bulk fuel bed (exterior area of particles), A_{VB}, as a function of mass remaining; this is calculable if the particle size and shape are well characterized but it can pose a problem with some fuels. The solid to gas transport coefficients K and H should be calculable from various packed bed correlations; the mass loss rate for the particles will probably be, in most cases of smoldering, too small to alter these values appreciably from those of inert particles.

Bulk Gas Equations. Regardless of whether the condensed phase requires single particle treatment or bulk treatment, the gas phase around the particles is treated here as a continuum without transverse gradients on the particle scale. The following set of bulk gas conservation equations is coupled to either of the two sets of solid equations given above in order to obtain a complete description of the smolder wave propagation process.

Conservation of gas mass in bulk gas phase:

$$\frac{\partial}{\partial t} (\phi \rho_G) + \overline{\nabla} \cdot (\overline{v}_G \rho_G \phi) = K \, A_{VB} \sum_{KG} (Y_{KGP} - Y_{KG}) \tag{17}$$

Here the gas is convecting (at velocity v_G) as a result of buoyancy or external pressure forces. The very slow gas movement that would be caused by drag from the shrinkage of the particle bed is neglected in this development. The source term on the right is the same as the last term (sink) in Eq. (12).

The mass fraction of component K in the particle (Y_{KGP} in last term) is evaluated at the particle/bulk gas phase interface.

Momentum of gas in bulk gas phase:

$$\phi \rho_G \frac{\partial \bar{v}_G}{\partial t} + \phi \rho_G (\bar{v}_G \cdot \bar{\nabla}) \bar{v}_G + \phi \bar{\nabla} P = - \phi \rho_G \bar{g} - c_1 \mu_G \bar{v}_G - c_2 \left(\bar{v}_{GX} |v_{GX}| + \bar{v}_{GY} |v_{GY}| \right)$$

$$-\bar{v}_G \left\{ K \, A_{VB} \sum_{KG} \left(Y_{KGP} - Y_{KG} \right) \right\} \tag{18}$$

Note that this is a vector equation obtained by summing x and y components. The gas continuity equation (Eq. (17)) has been substituted here introducing the acceleration term on the right hand side (last term). The second and third terms on the right hand side describe the flow drag caused by the fuel particles. This a two-dimensional differential form of the Ergun equation (78) applicable to laminar and turbulent flow. The parameters c_1 and c_2 are dependent on bed porosity and particle size; they are best measured empirically (by measurements of pressure drop versus flow rate on uniform beds of particles). In cases where a well-defined hydrostatic pressure gradient exists in the fuel bed, a perturbation pressure can be substituted for the total pressure P and its gradient used to convert the gravitational force term (first on right hand side) to a more familiar buoyancy term (79).

Conservation of typical gaseous species in bulk gas phase:

$$\phi \rho_G \frac{\partial Y_{jG}}{\partial t} + \phi \rho_G \bar{v}_G \cdot \bar{\nabla} Y_{jG} - \bar{\nabla} \cdot \left(\phi \rho_G D_{eB} \bar{\nabla} Y_{jG} \right) =$$

$$-K \, A_{VB} \left[\left(Y_{jG} - Y_{jGP} \right) + Y_{jP} \sum_{kG} \left(Y_{kG} - Y_{kGP} \right) \right] + \sum_m \left(\phi \left(\nu_F - \nu_C \right)_{mj} R_{mj} \right) \tag{19}$$

37

Again the gas continuity equation has been substituted introducing the dilu-
tion term on the right. The reaction term (last term) includes only homo-
geneous gas phase reactions. The diffusion term (third term) contains the
effective diffusivity of the various species in the bed, D_{eB}, assumed the same
for all species. In a packed bed, as the Reynolds number (based on particle
diameter) increases, the flow streamlines became increasingly complex due to
repeated splittings and diversions by the particles. The result is
effectively a mass transport process, dispersion (analogous somewhat to turbu-
lent eddies), that ultimately dominates over molecular diffusion but is
similarly described. Thus D_{eB} changes smoothly from an effective molecular
diffusivity to a dispersion coefficient with increasing Reynolds number (80).
An added complication, however, is that dispersion typically differs in direc-
tions parallel to the flow and transverse to the flow. The possible impact of
this should be considered in the context of a specific problem.

Conservation of gas energy in bulk gas phase:

$$\phi \rho_G \frac{\partial h_G}{\partial t} + \phi \rho_G \bar{v}_G \cdot \bar{\nabla} h_G - \bar{\nabla} \cdot \left(\phi \lambda_B \bar{\nabla} T_G\right) = -HA_{VB}\left(T_G - T_P\right)$$

$$+ K A_{VB} \sum_G \left(h_{KG} - h_G\right) \left(Y_{KGP} - Y_{KG}\right)$$

$$+ \sum_{KG} \left(h_{KG} \bar{\nabla} \cdot \left(\phi \rho_G D_{eB} \bar{\nabla} Y_{KG}\right)\right) + \sum_m \left(R_{mG} Q_{m,STP}\right) \tag{20}$$

Here Eqns. (17)-(19) have been substituted to obtain the form shown. Note
that, as in Eq. (16), bulk heat conduction (third term) is proportioned to
this phase in accord with the local fractional free volume (or area), ϕ .
This is a reasonable approximation for the general situation where local bulk

38

gas and bulk solid temperatures are unequal. Note that radiation in the gas is neglected on the assumption of short pathlengths and small emissivities. The other terms in Eq. (20) are analogous to similar terms in Eq. (7) or Eq. (16), explained previously. Again, kinetic energy, pressure work, drag work and gravity work are neglected. As before, various supplementary relations giving temperature and species dependence of thermal properties, etc., are needed to complete these equations.

A complete problem description requires the bulk gas phase equations (Eq. (17)-(20) plus supplementary relations), coupled to either the single particle equations (Eq. (2)-(7) plus supplementary relations plus interphase boundary conditions such as Eq. (8) and (9)) or the bulk solid phase equations (Eq. (10)-(16) plus supplementary relations). In addition one needs boundary and initial conditions on the bulk gas and bulk solid (if treated as such) for the particular fuel bed configuration of interest. It was noted previously that the gas phase around the fuel bed may, in some cases, be a closely coupled part of the total propagation problem. This could be particularly true when the smolder process induces a buoyant flow in the surrounding gas and the details of that flow have a strong influence on the rate of oxygen supply from the ambient air to the fuel bed. Since such buoyant flows themselves can pose a difficult problem, the fully coupled, ambient gas-plus-fuel bed situation has not been addressed. Instead, as a first approximation, the ambient gas is assumed to be homogeneous just as was the case with the single particle equations. Heat and mass transfer from the ambient air to the fuel bed are assumed to occur across a thin boundary layer with known heat and mass transfer coefficients. Appropriate boundary conditions on the bulk gas and the bulk solid will be analogous to Eq. (8) and (9), minus the surface

reaction terms; the bulk solid boundary condition would typically contain radiative exchange with the surroundings as well. Note that the use of the single particle equations (Eq. (2)-(7)) to describe the condensed phase does not permit application of fuel bed boundary conditions on the solid phase. The boundaries would then be felt by the solid only through its interaction with the bulk gas; this could yield a poor description of the solid thermal profile near the bed boundaries. This is the second area related to heat transfer on the smolder wave scale in which the use of the single particle equations poses problems. However, these problems can probably be avoided in most smolder problems of interest. As will be seen below, the condensed phase particle scale gradients of most frequent significance are in species and not temperature. If this is the case, the bulk condensed energy equation can be used to obtain the bulk solid temperature (with some further minor assumptions), assumed uniform throughout the typical particle, while the remaining single particle equations are used to correctly describe particle scale species gradients and reaction rates. Then the heat transfer problems associated with the single particle equations do not appear.

Non-Dimensionalization. The preceding sets of equations can be substantially simplified for specific problems once various parameter values have been defined. To facilitate the identification of situations where various terms can be neglected, the equations have been non-dimensionalized. The non-dimensionalization via the reference quantities in Table II is designed to render all important terms of order unity. The choice of reference quantities imposes some interrelationships among them. The expression in Table II for the reference bulk gas flow velocity v_{GR} comes from the assumption that flow drag and buoyancy are balanced in the bed of fuel

40

particles. The reference particle flow velocity (due to particle shrinkage), v_{PR}, is taken to be comparable to the smolder propagation velocity and estimated from the average equivalence ratio of the smolder wave assuming all oxygen is transported in at the flow velocity, v_{GR}. The expression for the reference length on the scale of the smolder wave, ℓ_R, comes from the assumption that heat conduction and convection are comparable in the particle bed. The reference time, t_R, is thus essentially of the order of the smolder wave passage time. The actual ranges of numbers used for these reference values (as listed in Table II) cover the spectrum seen experimentally in a wide variety of configurations (Table I plus some other cases as well).

The large set of dimensionless parameters in Table II is not necessarily the minimum number nor the optimum set for a specific problem. This set suffices to assess the relative importance of various terms in Eqns. (2)-(20) for a wide spectrum of smolder propagation problems.

The dimensionless set of conservation equations is as follows.

Conservation of gas mass in bulk gas phase (from Eq. (17)):

$$\pi_1 \frac{\partial(\hat{\rho}_G \hat{\phi})}{\partial \hat{t}} + \hat{\bar{\nabla}} \cdot \left(\hat{\bar{v}} \, \hat{\rho}_G \, \hat{\phi} \right) = \sum_{KG} \left(\pi_{2K} \left(\hat{Y}_{KGP} - \hat{Y}_{KG} \right) \right) \tag{21}$$

Conservation of x-momentum in bulk gas phase (x component, from Eqn. (18)):

$$\pi_3 \hat{\phi} \, \hat{\rho}_G \frac{\partial \hat{v}_x}{\partial \hat{t}} + \pi_4 \left(\hat{\rho}_G \, \hat{\phi} \, \hat{v}_x \frac{\partial \hat{v}_x}{\partial \hat{x}} + \hat{\rho}_G \, \hat{\phi} \, \hat{v}_y \frac{\partial \hat{v}_x}{\partial \hat{y}} \right) = -\hat{\phi} \frac{\partial \hat{P}'}{\partial \hat{x}} + \pi_5 \hat{\phi} \left(\frac{\hat{T} - \hat{T}_A}{\hat{T}} \right)$$

$$- \hat{\mu} \, \hat{v}_x - \pi_6 \, \hat{v}_x \, |\hat{v}_x| - \hat{v}_x \sum_{KG} \left(\pi_{7K} \left(\hat{Y}_{KGP} - \hat{Y}_{KG} \right) \right) \tag{22}$$

41

Here the ambient hydrostatic pressure gradient has been separated from the total pressure gradient term resulting in converting the gravity term to a buoyancy term (second term on right hand side), as discussed above. The y component of momentum is substantially the same as the x component in this general analysis so it is not considered separately.

Conservation of typical gaseous species in bulk gas phase (from Eq. (19)):

$$\pi_{8j} \; \hat{\phi} \; \hat{\rho}_G \; \frac{\partial \hat{Y}_{jG}}{\partial \hat{t}} + \hat{\phi} \; \hat{\rho}_G \; \hat{\bar{v}}_G \cdot \hat{\bar{\nabla}} \; \hat{Y}_{jG} - \pi_{9j} \; \hat{\bar{\nabla}} \cdot (\hat{\phi} \; \hat{\rho}_G \; \hat{D}_{eb} \; \hat{\bar{\nabla}} \; \hat{Y}_{jG}) =$$

$$- \pi_{2j} \; ((\hat{Y}_{jG} - \hat{Y}_{jGP}) + \sum_G \pi_{25K}(\hat{Y}_{KG} - \hat{Y}_{KGP})) + \sum_m (\pi_{10mj} \; \hat{R}_m) \qquad (23)$$

Conservation of gas energy in bulk gas phase (from Eq. (20)):

$$\pi_1 \; \hat{\phi} \; \hat{\rho}_G \; \frac{\partial \hat{h}_G}{\partial \hat{t}} + \hat{\phi} \; \hat{\rho}_G \; \hat{\bar{v}}_G \cdot \hat{\bar{\nabla}} \; \hat{h}_G - \pi_{11} \; \hat{\bar{\nabla}} \cdot (\hat{\phi} \; \hat{\lambda}_B \; \hat{\bar{\nabla}} \; \hat{T}_G) =$$

$$- \pi_{12} \; \hat{A}_{VB} \; (\hat{T}_G - \hat{T}_P) + \sum_{KG} \pi_{2K} \; (\hat{h}_{GK} - \hat{h}_G)(\hat{Y}_{KGP} - \hat{Y}_{KG})$$

$$+ \sum_{KG} (\pi_{9K} \; \hat{h}_{KG} \; \hat{\bar{\nabla}} \cdot (\hat{\phi} \; \hat{\rho}_G \; \hat{D}_{eb} \; \hat{\bar{\nabla}} \; \hat{Y}_K)) + \sum_m (\pi_{13m} \; \hat{R}_m) \qquad (24)$$

Conservation of void volume in the particle bed (from Eq. (10)):

$$\pi_{14} \; \frac{\partial \hat{\phi}}{\partial \hat{t}} - \hat{\bar{\nabla}} \cdot \left[\hat{\bar{v}}_P \; (1 - \pi_{15} \; \hat{\phi}) \right] = \pi_{17} \; \hat{\Lambda}_P \qquad (25)$$

Conservation of gas in bulk condensed phase (from Eq. (12)):

$$\pi_{19} \frac{\partial}{\partial \hat{t}}\left[\left(1 - \pi_{15}\,\hat{\phi}\right)\hat{\phi}_P\,\hat{\rho}_{GP}\right] + \pi_{20}\,\hat{\bar{\nabla}}\cdot\left[\hat{\bar{v}}_P\left(1 - \pi_{15}\,\hat{\phi}\right)\hat{\phi}_P\,\hat{\rho}_{GP}\right]$$

$$= \left(1 - \pi_{15}\,\hat{\phi}\right)\hat{R}_1 + \left(1 - \pi_{15}\,\hat{\phi}\right)\sum_{\ell>1}\left(\pi_{21\ell}\,\hat{R}_\ell\right)$$

$$- \sum_{KG}\left(\pi_{22K}\left(\hat{Y}_{KGP} - \hat{Y}_{KG}\right)\right) \tag{26}$$

Here, and in other equations below, the first chemical reaction term in the condensed phase (subscript 1) has been assumed to be among the largest and its reference rate (RR_1) is used to normalize the other terms in the equation; thus it stands out of the summations over condensed phase reaction rates.

Conservation of solid in the bulk condensed phase (from Eq. (13)):

$$(\pi_{14}/\pi_{15})\,\frac{\partial}{\partial \hat{t}}\left[\left(1 - \pi_{15}\,\hat{\phi}\right)\left(1 - \pi_{16}\,\hat{\phi}_P\right)\hat{\rho}_P\right] + \hat{\bar{\nabla}}\cdot\left[\hat{\bar{v}}_P\left(1 - \pi_{15}\,\hat{\phi}\right)\left(1 - \pi_{16}\,\hat{\phi}_P\right)\hat{\rho}_P\right]$$

$$= -\left(1 - \pi_{15}\,\hat{\phi}\right)\sum_{\ell}\left(\pi_{18\ell}\,\hat{R}_\ell\right) \tag{27}$$

Conservation of typical gas species in bulk condensed phase (from Eq. (14)):

$$\pi_{23j}\left(1 - \pi_{15}\,\hat{\phi}\right)\hat{\phi}_P\,\hat{\rho}_{GP}\,\frac{\partial \hat{Y}_{jGP}}{\partial \hat{t}} + \pi_{24j}\left(1 - \pi_{15}\,\hat{\phi}\right)\hat{\phi}_P\,\hat{\rho}_{GP}\,\hat{\bar{v}}_P\cdot\hat{\bar{\nabla}}\,\hat{Y}_{jGP} =$$

$$\left(1 - \pi_{15}\,\hat{\phi}\right)\left(\pi_{25j1} - \pi_{26j}\right)\hat{R}_1 + \left(1 - \pi_{15}\,\hat{\phi}\right)\sum_{\ell>1}\left(\left(\pi_{25\ell j} - \pi_{26j}\right)\pi_{21\ell}\,\hat{R}_\ell\right)$$

$$- \pi_{22j}\left[\left(\hat{Y}_{jGP} - \hat{Y}_{jG}\right) - \hat{Y}_{jGP}\sum_{KG}\left(\pi_{26K}\left(\hat{Y}_{KGP} - \hat{Y}_{KG}\right)\right)\right] \tag{28}$$

43

Conservation of typical solid species in bulk condensed phase (from Eq. (15)):

$$(\pi_{14}/\pi_{15}) \; \hat{\rho}_P \; \frac{\partial \hat{Y}_{KP}}{\partial \hat{t}} + \hat{\bar{v}}_P \cdot \hat{\bar{\nabla}} \hat{Y}_{jP} = \left(1/\left(1 - \pi_{15} \hat{\phi}\right)\right) \sum_{\ell} \left(\pi_{18\ell j} \left(\pi_{25\ell j} + \pi_{26 j}\right) \hat{R}_\ell\right)$$

(29)

Conservation of gas/solid energy in bulk condensed phase (from Eq. (16)):

$$\left(1 - \pi_{15} \hat{\phi}\right) \left[(\pi_{14}/\pi_{15}) \; \pi_{28} \; \hat{\phi}_P \; \hat{\rho}_P \; \frac{\partial \hat{h}_{GP}}{\partial \hat{t}} + \left(1 - \pi_{16} \hat{\phi}_P\right)(\pi_{14}/\pi_{15}) \; \hat{\rho}_P \; \frac{\partial \hat{h}_P}{\partial \hat{t}} \right.$$

$$\left. + \pi_{27} \; \hat{\phi}_P \; \hat{\rho}_{GP} \; \hat{\bar{v}}_P \cdot \hat{\bar{\nabla}} \hat{h}_{GP} + \left(1 - \pi_{16} \hat{\phi}_P\right) \hat{\rho}_P \; \hat{\bar{v}}_P \cdot \hat{\bar{\nabla}} \hat{h}_P \right]$$

$$- \hat{\bar{\nabla}} \cdot \left[\left(1 - \pi_{16} \hat{\phi}_P\right) \hat{\lambda}_P \; \hat{\bar{\nabla}} \hat{T}_P \right] + \pi_{28} \; \hat{\bar{\nabla}} \cdot \hat{\bar{S}} = \pi_{29} \; \hat{A}_{VB} \left(\hat{T}_G - \hat{T}_P\right)$$

$$+ \left(\hat{h}_G - \hat{h}_{GP}\right)\left(1 - \pi_{15} \hat{\phi}\right) \sum_{\ell} \left(\pi_{18\ell} \; \hat{R}_\ell\right) + \sum_{KG} \pi_{30K}\left(\hat{Y}_{KGP} - \hat{Y}_{KG}\right)\left(\hat{h}_{GP} - \hat{h}_{GK}\right)$$

$$+ \left(1 - \pi_{15} \hat{\phi}\right) \sum_{\ell} \left(\pi_{31\ell} \; \pi_{18\ell} \; \hat{R}_\ell\right)$$

(30)

Alternatively, if the particle phase has species and temperature gradients on the scale of a single particle, Eq. (2)-(9) apply instead of Eq. (10)-(16) and the former equations, when non-dimensionalized via the reference quantities in Table II, become as follows.

Conservation of gas mass within particle pores (from Eq. (2)):

$$\pi_{32} \frac{\partial}{\partial \hat{t}} \left(\hat{\phi}_P \; \hat{\rho}_{GP}\right) + \pi_{33} \frac{1}{\hat{r}^a} \frac{\partial}{\partial \hat{r}} \left(\hat{r}^a \; \hat{\rho}_{GP} \; \hat{\phi}_P \; \hat{v}_{GP}\right) = \hat{R}_1 + \sum_{\ell > 1} \left(\pi_{21\ell} \; \hat{R}_\ell\right)$$

(31)

Conservation of solid mass within particle (from Eq. (3)):

$$\pi_{34} \frac{\partial}{\partial \hat{t}} \left[\left(1 - \pi_{16} \hat{\phi}_P\right) \hat{\rho}_P \right] = -\hat{R}_1 - \sum_{\ell > 1} \left(\pi_{21\ell} \hat{R}_\ell\right) \tag{32}$$

Conservation of momentum of gas in particle pores (from Eq. (4)):

$$\pi_{35} \hat{\phi}_P \hat{\rho}_{GP} \frac{\partial \hat{v}_{GP}}{\partial \hat{t}} + \pi_{36} \hat{\phi}_P \hat{\rho}_{GP} \hat{v}_{GP} \frac{\partial \hat{v}_{GP}}{\partial \hat{r}} = -\hat{\phi}_P \frac{\partial \hat{P}_P}{\partial \hat{r}} - \hat{\mu}_{GP} \hat{v}_{GP} - \hat{v}_{GP} \sum_{\ell} \left(\pi_{37\ell} \hat{R}_\ell\right) \tag{33}$$

Conservation of typical gas species in particle pores (from Eq. (5)):

$$\pi_{39j} \hat{\phi}_P \hat{\rho}_{GP} \frac{\partial \hat{Y}_{jGP}}{\partial \hat{t}} + \pi_{40j} \hat{\phi}_P \hat{\rho}_{GP} \hat{v}_{GP} \frac{\partial \hat{Y}_{jGP}}{\partial \hat{r}} - \pi_{41j} \frac{1}{\hat{r}^a} \frac{\partial}{\partial \hat{r}} \left(\hat{r}^a \hat{\rho}_{GP} \hat{D}_{ep} \frac{\partial \hat{Y}_{jGP}}{\partial \hat{r}} \right)$$

$$= \left(\pi_{24j1} - \pi_{25j}\right) \hat{R}_1 + \sum_{\ell > 1} \left[\left(\nu_F - \nu_C\right)_{\ell j} - \pi_{25j} \hat{Y}_{jGP} \right] \pi_{21\ell} \hat{R}_\ell \tag{34}$$

Conservation of typical condensed phase species in particle (from Eq. (6)):

$$\left(1 - \pi_{16} \hat{\phi}_P\right) \pi_{38j} \hat{\rho}_P \frac{\partial \hat{Y}_{jP}}{\partial \hat{t}} = -\hat{R}_1 - \sum_{\ell > 1} \left(\pi_{21\ell} \hat{R}_\ell\right) \tag{35}$$

Conservation of gas and solid energy in particle (from Eq. (7)):

$$\pi_{44} \left(1 - \pi_{16} \hat{\phi}_P\right) \hat{\rho}_P \frac{\partial \hat{h}_P}{\partial \hat{t}} + \pi_{45} \hat{\phi}_P \hat{\rho}_{GP} \frac{\partial \hat{h}_{GP}}{\partial \hat{t}} + \pi_{46} \hat{\phi}_P \hat{\rho}_{GP} \hat{v}_{GP} \frac{\partial \hat{h}_{GP}}{\partial \hat{r}}$$

$$- \pi_{47} \frac{1}{\hat{r}^a} \frac{\partial}{\partial \hat{r}} \left(\hat{r}^a \hat{\lambda}_P \frac{\partial \hat{T}_P}{\partial \hat{r}} \right) - \frac{1}{\hat{r}} \frac{\partial}{\partial \hat{r}} \left[\sum_{KG} \left(\pi_{48K} \hat{h}_{KGP} \hat{\rho}_{GP} \hat{D}_{ep} \hat{r} \frac{\partial \hat{Y}_{KGP}}{\partial \hat{r}} \right) \right]$$

$$= \left[1 + \pi_{49} \left(\hat{h}_P - \hat{h}_{GP} \right) \right] + \sum_{\ell > 1} \left[\pi_{50\ell} \left(1 + \pi_{51\ell} \left(\hat{h}_P - \hat{h}_{GP} \right) \right) \right] \tag{36}$$

The two boundary conditions of principal interest at the exterior particle surface become (from Eq. (8) and (9)):

$$-\pi_{54}\hat{\phi}_P\hat{\rho}_{GP}\hat{v}_{GP}\hat{Y}_{jGP} - \pi_{42}\hat{\phi}_P\hat{\rho}_{GP}\hat{D}_{ep}\frac{\partial\hat{Y}_{jGP}}{\partial\hat{r}} = \left(\hat{Y}_{jGP}-\hat{Y}_G\right) + \left(1-\pi_{16}\hat{\phi}_P\right)\sum_\ell\left(\pi_{43\ell j}\hat{R}_\ell\right) \quad (37)$$

$$\pi_{52}\hat{\lambda}_P\frac{\partial\hat{T}_P}{\partial\hat{r}} + \left(\hat{T}_P - \hat{T}_G\right) = \left(1 - \pi_{16}\hat{\phi}_P\right)\sum_\ell\left(\pi_{53\ell}\hat{R}_\ell\right) + \pi_{55}\hat{\phi}_P\hat{\rho}_{GP}\hat{v}_{GP}\hat{h}_{GP} \quad (38)$$

It should be noted that in the preceding non-dimensionalization process, all reaction terms, whether in the bulk gas phase or on the particle surface, were assumed to have power law species dependencies and an Arrhenius temperature dependence; this form is mirrored in the definition of RR_ℓ (see $\pi_{18\ell}$ in Table II). Many char gasification reactions are more aptly described by a Langmuir-Hinshelwood kinetic rate law which is somewhat more complex but behaves like a power law over limited species concentration ranges (52, 81).

In Eqns. (21) to (38) all wave-scale gradients are of order unity as are the time derivatives. Transverse gradients $(\partial/\partial\hat{r})$ in the single particle equations are to be assessed as are their analogs in the bulk gas and solid equations, i.e., terms involving a difference between bulk gas and bulk solid species concentration or temperature. The dimensionless reaction rates $\hat{R}_m$ in the bulk gas phase and $\hat{R}_\ell$ on the particle surface are of order unity for the principal reactions of interest when $\hat{T}$ approaches unity. The net result is that all symbols with a caret above them denoting a non-dimensionalized value are of order unity; the relative importance of each term in a given equation then is indicated by the magnitude of the π group it includes. For the transverse gradient terms first mentioned, the situation is somewhat more complex, as will be discussed.

46

<u>Magnitude of Dimensionless Groups and Simplifications</u>. First, note that
in all of the dimensionless equations involving a time derivative of a gas
phase variable (exclude Eq. (25), ϕ is not really a gas phase variable) the
π's are small, typically 10^{-3} or less (see π_1, π_3, π_{8j}, π_{19}, π_{23j}, π_{27}, π_{32},
π_{35}, π_{39j}, and π_{45} in Table II). This implies that, to a good approximation,
these transient gas terms can be neglected; the bulk gas as well as the gas
within the condensed phase can be treated as quasi-steady. This is a conse-
quence of the large disparity in densities between the gas and condensed
phases as well as of the chosen time scale here, i.e., the wave passage time.
If rapid ignition or other fast transient was of interest, the storage
capacity of the gas phase could become significant.

The solid/gas density discrepancy also renders negligible the gas
convecting with the bulk condensed phase (in its pores; second term in
Eq. (26) and (28); third term in Eq. (30)). Note that the corresponding π's
(π_{20}, π_{24j} and π_{27}) are all of order 10^{-3} so these terms can be neglected with
the same degree of accuracy as that in the quasi-steady gas phase assumption.
(This does not apply to the gas convection in the single particle equations
since it can be occurring at a much higher velocity.)

The preceding approximations leave Eq. (26) and (28) with only two types
of terms, mass (or species) generation by reaction and mass (or species)
transfer across the external boundary layer around the condensed phase
particles. These terms must balance each other. Eq. (26) reduces to the
algebraic statement that the net mass transfer rate equals the net particle
gasification rate. Eq. (28) with the aid of Eq. (26), reduces to the alge-
braic statement that the rate of mass transfer of a typical species to or from

the condensed phase equals its net rate of consumption or production by the surface reactions in the particle phase. If this algebraic equality is solvable for the concentration of the species of interest in the condensed phase (e.g., that of oxygen, if the reaction is first order in oxygen mass fraction), this relation can be used to eliminate that unknown concentration elsewhere in the model equations (82).

The gas momentum equations (Eq. (22) and (33)) can usually be simplified. Table II shows that the π's multiplying the acceleration terms (π_4, π_{7K} in Eq. (22); π_{36}, $\pi_{37\ell}$ in Eq. (33)) can be small or of order unity. Most realistic cases are expected to make these terms small. Only a fuel bed with a very open structure, producing a low flow drag, while still sustaining a compact smolder wave would yield significant acceleration effects in Eq. (22). The conditions for significant acceleration effects in single particles are analogous--rapid gasification out of small particles with very open, low flow drag pores. Typically only the drag, pressure gradient and buoyancy (bulk gas only) terms need be retained (see π_5 and π_6). Even the turbulent part of the flow drag is typically small unless the Reynolds number of the particles exceeds 10 or so (83) and it is not even included for flow in the particle pores (Eq. (33)).

The preceding approximations can be expected to apply to most smolder propagation models. Their validity in specific applications should always be checked, however.

Note that the π's multiplying the interphase transport terms (π_{2K}, π_{12}, π_{22j}, π_{29}, π_{30K}) have a very large potential range of values as shown in

Table II. The mass and heat transfer coefficients used to evaluate these π's are based on standard packed bed correlations (73). These transport processes must always be occurring at a significant rate in this type of problem, thus, the terms in the equations which describe them must be of order unity. This implies that when the π value in the term is large, the temperature or mass fraction difference in the term must be small and conversely. Thus, if π_{12} and π_{29} are large, the temperature difference between the bulk gas and the bulk solid must be small. If it is sufficiently small as to have no significant effect on the reaction rates, there is no real need to keep track of this difference. The bulk gas and bulk solid energy equations can be combined yielding a single local temperature to be tracked. Because of the close analogy between heat and mass transfer, one might expect the temperature and mass concentration differences between the two phases to be small or large in similar conditions. In the reaction zone, however, if the condensed phase reactions are the major cause of the temperature difference between phases, the temperature difference will tend to be larger than the concentration difference (111). In any event, when π_{2K}, π_{22j} and π_{30K} are large compared to unity, the concentration differences are also small and it becomes unnecessary to separately track a bulk gas phase and bulk condensed phase oxygen mass fraction, for example.

For cases with internal gradients in the particles, the interphase transport coefficients show up in π_{42} and π_{52} in Eqns. (37) and (38); variations in their values have somewhat different implications. Recall that the boundary layer heat and mass transfer resistances are in series with those in the particle. A large value of π_{52} means that the heat conduction in the particle is much faster than heat transfer across the boundary layer around

49

the particle. Then the temperature within the particle will be nearly uniform
but it will differ appreciably from the surrounding bulk gas. If so, Eq. (30)
can take the place of Eq. (36). The converse case, small π_{52}, affords no
simplification; it merely means the bulk gas and particle surface temperatures
are nearly equal. Note that the range of expected values for π_{52} is biased
toward values greater than unity; typical fuel particles smaller than about
1 cm tend to satisfy this criterion for uniform internal temperature. Similar
reasoning applies to π_{42} so that large values would again imply uniformity,
this time of gas species concentrations, within the particle pores. Table II
shows, however, that the range of expected values for π_{42} is biased strongly
toward values much less than unity. This is a consequence of the small
diffusivities likely to be encountered in particle pores. Thus temperature
uniformity is much more likely than species uniformity in the particles as a
consequence of slow external transport. Even when external transport
considerations such as these do not yield diminished gradients in the
particles, the gradients may still be small, as shown below.

The single particle equations show that gas species within the pores can
move by both convection and diffusion. The convection is due to the self-
generated internal pressure gradient in the particles as a result of their
gasification. The species of interest are those that affect the reaction
rates within the particle; oxygen is of primary interest but CO_2, CO, H_2 and
H_2O could be pertinent in high temperature cases, as discussed previously.
Oxygen must diffuse in against the net outward flow. Internally generated
species both diffuse and flow outward. The absolute and relative magnitudes
of π_{40j} and π_{41j} in Eq. (34) indicate the importance of convection and diffu-
sion of the typical species. Note that π_{40j} was evaluated using the maximum

50

value of V_{GPR} (i.e., assuming that flow alone carries all of the gasified mass from the particle) so that π_{40j} is less than or, at most, equal to unity. On the other hand π_{41j} may be very small (large particles, small pores) or very large (small particles, large pores). Suppose that π_{41j} is much greater than unity. Since the total diffusion term will be of order unity at most (to balance the reaction rate), then the species gradient which causes diffusion must be proportionately much less than unity. This implies the species gradient can be neglected and Eq. (28) can be used in place of Eq. (34). Conversely, suppose that π_{41j} is much less than unity (and π_{40j}). Then diffusion is restricted and convective flow may play an important role in species movement. The diffusion term does not drop out of the problem since the species gradient for an incoming gas can become greater than unity. Thus oxygen, diffusing in against the convective outflow penetrates only a fraction of the particle diameter. In the extreme limit, the oxygen cannot penetrate the pores significantly and oxidation reactions are confined to the outer surface of the particle. This is analogous to Zone III behavior but we have the added complication of the outward flow of gases contributing to it. If these gases originate in an oxygen-free region of the particle, they must come from the pyrolytic reactions. This behavior is most likely to be encountered in the pyrolysis portion of a fast moving smolder wave when the initial fuel particles are large and have no pores or only very small pores. Note, then, that these physical effects can shift the competition between pure pyrolysis and oxidative pyrolysis; if oxygen cannot penetrate the pore system, oxidative pyrolysis is confined to the particle exterior while pure pyrolysis is uninhibited. In sections of the smolder wave where such pyrolysis is minimal or negligible (i.e., where char oxidation is occurring), the gasification process will essentially cease in portions of the particle where oxygen does

51

not penetrate and the net convective outward flow will be due only to the oxidation reactions. Zone III behavior in this case involves no flow from within the particles; it erodes from the exterior (shrinking core) and all of the internal species and flow equations can be dropped.

Similar considerations regarding convective and conductive heat transfer within a particle are influenced by the values of π_{46} and π_{47}. A value of π_{47} that is much greater than unity implies that the temperature gradient in the particle is much less than unity and, thus, Eq. (36) can be replaced by Eq. (30). Conversely, π_{47} much less than unity implies large temperature gradients so that conduction still may be important. Convection is important only if diffusion is unable to remove the products rapidly (small π_{40K}, as above). If convection is not important, the flow equation for the particle interior can be dropped.

Note that π_{41j} has a greater potential range of values below unity than does π_{47}. This is again due to the possibility of restricted diffusion in pores; the pores typically have no great effect on the thermal conductivity or thermal diffusivity of the solid particles. One can infer from this that smolder problems with significant internal species gradients in the particles but negligible temperature gradients will be encountered more frequently than problems with both types of gradient. Recall that a similar conclusion was reached when examining the influence of external transport limitations. Of course, if the species and temperature gradients are both small, the single particle equations are not needed.

52

Laurendeau (52) presents a further argument to the effect that temperature gradients can frequently be neglected. Originally derived for catalyst particles, it pertains here to fuel particles in which only char oxidation is occurring. It also pertains here only to cases in which π_{44} is at the low end of its range in Table II since the assumption is made that transient thermal processes in the particle are negligible. Given these restrictions, one can estimate the temperature gradient within a particle by balancing heat conducted out of the particle against char oxidation heat generation; the latter is limited by the rate of oxygen inward diffusion in the regime of interest. The final result becomes

$$\beta_T \equiv ((T_{PC} - T_{PS})/T_{PS}) = -\left(\frac{D_{ep}\rho_{GP}Y_{OXS}Q_{CO}}{\lambda_P T_{PS}}\right) \tag{39}$$

Here β_T is the fractional variation in particle temperature (difference between center and surface temperatures (T_{PC} and T_{PS}, respectively), divided by the surface temperature), Y_{OXS} is the oxygen mass fraction at the particle surface and Q_{CO}, the heat of the char oxidation process. Even for fairly large pores (500Å) the value of β_T computed above is likely to be less than 0.05. Laurendeau quotes studies showing that $\beta_T < 0.05$ typically yields results quite similar to isothermal particles.

A few other simplifications in the single particle equations are possible. Inspection of Table II shows that π_{36} and $\pi_{37\ell}$ in Eq. (33) can be much less than unity (and almost always are); these acceleration terms can then be dropped from the momentum equations leaving a balance between the self-generated pressure gradient and laminar flow out through the particle pores. The last term on the left hand side of Eq. (36) describes the net

53

enthalpy transported by diffusion. While Table II shows that π_{48K} may be small or large, it is probable that the algebraic sum of diffusive enthalpy fluxes represented here will be small unless one species has an exceptional specific enthalpy. Neglecting this term should give the same degree of approximation as that already included in the assumption of equal diffusivities for all species. The surface reaction terms in Eq. (37) and (38) are typically either dominant (non-porous particles) or negligible (typical porous particles); they should be retained or dropped accordingly.

All of the preceding assumed that the fuel particles are of a single size. In the absence of internal gradients, it does not really matter if this is so or not (unless the oxidation reactions are confined to the exterior surface of the particles). However, if there are internal gradients, a distribution of particle sizes can add substantial complexity in behavior. If the largest particles are not small compared to the smolder wave length in regions of average or smaller particles, the smolder front becomes inherently three-dimensional and untreatable by the continuum assumption used here. Qualitatively, one can envision the behavior of such a system. Large particles take longer to be gasified than small particles when the internal gradients are significant (Zone II or Zone III behavior). The smolder front would tend to move ahead and to surround large particles ultimately leaving very large particles behind to be slowly consumed or quenched. Similar qualitative behavior can be exhibited by a fuel bed of small particles which are very unevenly packed, i.e., regions of higher packing density (and lower permeability) can mimic the behavior of very large particles.

If there is a distribution of particle sizes, at least some with internal gradients, and they are all small enough to satisfy the continuum wave assumption, the approach here can be used, in principle. Recall, however, that the boundary conditions (Eq. (8) and (9) or (37) and (38)) apply at the particle radius which is different for each segment of the size distribution. This implies a need to solve the single particle equations for each particle size increment of interest at each station along the smolder wave at each time step--a virtually hopeless task. In fact the numerical solution task is daunting even for a single particle size and, as will be seen, it has not yet been attempted in the context of smolder propagation. Qualitatively we can again envision the behavior. The smallest particles will meet the criteria for Zone I behavior; there will be no significant temperature or species gradients within these particles and they will be consumed first at a rate dictated by the reaction chemistry. Somewhat larger particles will most probably have significant species gradients but a uniform internal temperature. Still larger particles will have species and temperature gradients; the largest of these will be consumed last at a rate heavily dependent on heat and mass transfer processes (possibly including external transport processes).

Approaches Used With Some Related Problems. The formidable nature of a packed bed reactor problem with internal gradients in the particles has long been recognized. This problem appears in catalyst beds, blast furnaces, various ore treatment processes, incinerators and in coal and oil shale retorting. A widely used approach is to develop an analytical description of the behavior of a single particle and then to place this model of a typical particle into the context of the spatially varying surroundings (temperature, reactant gases) produced by the reaction wave progressing through the particle array.

55

Single particle reaction models are discussed extensively in Refs. 52 and 73. Virtually all analytical models are based on isothermal particles and the pseudo-steady-state approximation (as was used to obtain Eq. (39)). Laurendeau (52) summarizes the essence of various classes of models. External diffusive transport can be controlling (Zone III behavior); for a spherical particle this leads to a particle consumption time proportional to the square of the initial diameter. If external transport is not rate limiting, attention turns to processes at the exterior particle surface or within the particle pores. Laurendeau separates these models into macroscopic and microscopic types. The simplest macroscopic model ignores pores in the fuel and considers only reaction on the progressively shrinking external surface of the particle; reactant diffusion through any ash residue may also need to be considered. The more general macroscopic models consider the distribution of reaction throughout the particle as a result of reactant diffusion in through pores. Laurendeau indicates that the major practical difficulty with such models is inadequate information on the evolution of the effective reactant diffusivity in the pore system as it changes through the course of particle consumption. Microscopic models focus typically on a single "representative" pore and model its evolution with extent of reaction; more sophisticated models consider a distribution of pore sizes. The chemistry in all of these analytical models is typically restricted to a single nth order gasification reaction. Szekely et al (73) present a more extensive development of such models and also discuss the use of such models in the context of a bed of fuel particles.

In the context of smoldering combustion, it appears that such analytical modeling of events in a fuel particle interior could be applied to problems

(or segments of problems) where the only process in the particle interior is char oxidation. Such application has not yet been made but this approach should find application to some practical smolder problems in the future. The most general smolder case in which the fuel particle may undergo volumetric pyrolysis that generates a pore system coupled with oxygen diffusion leading to oxidative pyrolysis is probably not well enough defined yet to facilitate any truly detailed modeling.

Forward and Reverse Smolder Propagation. The behavior elicited from the preceding model equations is strongly dependent on the boundary conditions imposed. Most real world smolder propagation problems involve fuel beds immersed in air with oxygen penetrating the bed by diffusion and flow, as in Fig. 1, producing a two- (or three-) dimensional smolder reaction wave. Clearly it is preferable to begin exploring the behavior of these equations with simpler configurations, preferably one-dimensional (1-D) on the smolder wave scale. This requires that the smolder front and gas movement are parallel and that the smolder wave thickness is small compared to any general curvature of the smolder front.

There are two somewhat simpler limiting cases implicit in the preceding model equations that have received most attention, since they can be treated as one dimensional. The smolder reaction wave can move parallel to and in the same direction as the flux of oxygen (one-demensional forward smolder) or it can move in the opposite direction (one-dimensional reverse smolder). An observer moving with the reaction front sees a counter-current reactor in the forward smolder case (fuel and air come from opposite directions); reverse smolder propagation yields a co-current reactor (fuel and air come from the

same direction). The impact of this difference in relative directions of movement can be considerable. Figure 3 shows a qualitative comparison of wave-scale oxygen and temperature profiles for these two cases. This is drawn from the experimental work of Ref. (18) on smolder in beds of wood fibers but a similar result could be inferred from the in situ coal gasification literature.

The reverse smolder profiles are distinctly more simple. If one moves with the smolder front, the air and fuel enter the reaction zone intermingled with each other (though moving at different rates) and they can begin to react together as soon as the local temperature is elevated by heat transferred from the hotter regions. The wave resembles a laminar pre-mixed flame in this sense. As with a laminar flame, steady (or virtually steady) propagation is possible. Oxidation and pyrolysis reactions co-exist, competing for the condensed phase on the basis of their relative kinetic rates (assuming that transport limitations on the fuel particle scale do not enter in).

The forward smolder wave, on the other hand, seems to consist of several distinct zones. At the front of the wave (right side in Fig. 3) there is a plateau between a leading water condensation region and a trailing water evaporation region. All the water driven out of previously smoldered fuel, or formed from it, is trapped in this region which grows in length as the smolder wave progresses. (Other reversibly condensible materials can similarly accumulate but are usually much less prevalent.) DeRis (84) has pointed out, in a different context, that the net heat sink across this plateau is simply equal to the rate of sensible enthalpy accumulation in the material within the growing plateau region. The pyrolysis zone immediately following the plateau

58

is a major heat sink; note the lack of oxygen in this region for forward

smolder. This pyrolysis front moves forward into virgin fuel as rapidly as

heat transfer processes allow though it is ultimately limited by the fact that

the heat being absorbed here is generated in the char oxidation region at the

left. All oxygen consumption and heat generation occur at the left as the

entering oxygen attacks the pre-heated residue (char) from the pyrolysis

region. For the usual modest oxygen flow rates, this oxidation zone can only

move forward after it has consumed all the fuel (char) locally so that oxygen

can reach the next element of fuel. This links the rate of movement of the

char oxidation zone directly to the oxygen supply rate and the char oxidation

stoichiometry. Thus the heat generation zone and the heat sink zone

(pyrolysis + water plateau) move forward at what are, in general, differing

rates. Typically the pyrolysis front moves faster and a hot region builds

between them (unsteady behavior). In the absence of heat losses, this is a

major sink for the net heat generated; the remainder must exit with whatever

solid residue (e.g., ash) is left by the oxidation zone. A substantially

simplified solution for forward propagation of an exothermic reaction in the

absence of pyrolysis as a heat sink (85) shows that the peak temperature tends

to increase indefinitely; this is particularly rapid when the heat generation

zone moves forward at the same rate as the heat flow (convection dominated

case). In the more general case of Fig. 3, the pyrolysis front cannot consume

heat faster than it is generated in the oxidation region and the relative

rates of movement should tend toward the ratio of the net specific reaction

heats for each zone (assuming no heat losses and a diminishing heat content in

the oxidation zone residue).

It was found in Ref. (18) that the differing wave structures of Fig. 3 lead to differing oxidation chemistry dominating the propagation process, at least for the wood fibers studied there. In forward smolder, oxidation of the char residue from the pyrolysis zone must dominate, as noted above. In reverse smolder, this char is present in the reaction zone along with oxygen and the degrading fuel. The oxidation kinetics of this wood fiber char were found to be much slower than the oxidative pryolysis reactions which form the char (first DSC exotherm as discussed in section on Smolder Chemistry). The char was thus left behind intact by passage of the reverse smolder wave. Thus the forward/reverse differences can include not only alterations in temperature and oxygen profiles but also a complete shift in the nature of the dominant oxidation chemistry.

Purely forward and purely reverse smolder propagation are quite rare in the fire safety context. These pure combustion modes are found in other areas such as in situ coal gasification and oil shale retorting. Forward and reverse smolder are of interest here because their one-dimensional versions provide the simplest smolder propagation configurations for detailed modeling. Also, portions of realistic fire safety problems may approximate these simplest propagation modes. The smolder configuration in Fig. 1 is more typical of real world fire safety problems. This can be viewed as coupled forward and reverse smolder zones since oxygen enters the reaction zone from ahead of the wave permitting an exothermic oxidative pyrolysis process (reverse smolder zone); oxygen also enters from above and behind permitting exothermic char oxidation (forward smolder zone) (24).

60

In view of the preceding discussion one can suggest a logical progression of increasingly more complex and complete modeling efforts that would build ultimately to quantitative solutions to the general model equations above. The sequence is as follows: (1) One-dimensional reverse smolder with no internal gradients on the particle scale. Since this problem resembles a familiar deflagration wave, it is probably the simplest starting point. Comparisons with experiment are fairly easy; one-dimensional behavior can be approached if the smolder wave thickness is small compared to its radius of curvature. (2) One-dimensional forward smolder with no internal, particle-scale gradients. This case exhibits a more complex wave structure. It is also more difficult to produce experimentally; the transient growth in the total wave thickness demands an increasingly large fuel bed diameter to permit a one-dimensional wave front (18). Both of these experimental simulations are most readily done with forced air flow but the case of buoyant flow plus diffusive oxygen supply is also of interest as a prelude to the next stage in the modeling sequence. (3) Two-dimensional smolder propagation with no particle-scale gradients (cases such as that in Fig. 1). Such cases with a buoyant/diffusive oxygen supply are a mix of forward and reverse smolder behavior; they are found in many real-world situations. Various modes of simulating the coupling to the surrounding gas phase would require study at this point. (4) One-dimensional reverse smolder with particle scale gradients (single size particles); species-only gradients would cover many realistic fuels. (5) One-dimensional forward smolder with particle scale gradients; again, gradients in species alone would cover many real world fuels. (6) Two-dimensional smolder with particle scale gradients; this would require solutions to Eq. (2)-(9) and Eq. (17)-(20) with varying simplifications, as discussed above, depending on the area of application.

61

The numerical task becomes increasingly forbidding as one follows this
sequence. Bearing in mind that these models describe the coupling of thermo-
physics and chemistry, one cannot justify proceeding too far along this path
without better descriptions of the chemical rate processes than are presently
available. As will be seen, at present only steps (1) and (2) of this
suggested sequence have been partially explored.

Smolder Propagation Models in the Literature

Phenomenological Models. There have been only a few efforts to take
various sub-sets of the preceding equations and solve them fully as descrip-
tions of particular types of smolder problems. Before describing these it is
of interest to briefly mention some phenomenological models of smolder propa-
gation that have appeared in the literature. In most of these, an attempt is
made to derive a simple algebraic relation typically showing the dependence of
smolder velocity on other parameters; the basis is usually a heat balance,
greatly simplified.

Cohen and Luft (19) measured smolder propagation velocities through a
variety of materials in a horizontal layer configuration like Fig. 1. They
attempted to correlate these results with a qualitative, empirical model. The
model is based on a macroscopic one-dimensional balance of conductive and
convective heat transfer in the bed and the assumption that the air supply is
determined by a buoyancy/drag balance in the bed. No consideration is given
to a diffusive oxygen supply even though it is probably totally dominant for
the thin layers examined ($\leq$ 2 cm). A variety of parametric dependencies are
predicted but not adequately tested; some of the inferred and some of the

measured numbers are implausibly low (2-10% total solids gasification inferred; measured peak smolder zone temperatures as low as 165°C).

Kinbara, Endo and Sega (20) did a series of experiments on downward smoldering in vertical rods of various materials, mainly densely packed cellulosics. Their initial model was later refined by Sega, who also did additional similar experiments (86, 87). The emphasis in the modeling is on explaining the observed dependence of downward propagation velocity on sample width and on ambient temperature. The basis of the model is the one-dimensional steady state heat conduction equation for the bulk condensed phase; the principal approximations (besides the 1-D description of a 2-D problem) concern the rate of heat generation and heat loss along the reacting solid surface (roughly cone-shaped); both are linearized, the former on the assumption that heat generation is limited by oxygen transport to the reacting surface. In the original paper an unclear argument is used to infer, from an analytical solution of the heat equation, a smolder velocity expression with similar sample width and ambient temperature dependencies to those seen experimentally. Sega (87) later offered a more plausible derivation of a similar expression; similar approximate descriptions of heat generation and heat losses were used, however.

Williams (88) briefly discussed smolder propagation in a review of fire spread mechanisms. One-dimensional arguments are applied in a very broad manner not really addressed to any specific problem. For forward smolder a hypothesized balance between an oxygen-diffusion-limited rate of heat release and convective heat-up of the fuel (no heat losses) leads to a linear relation between smolder velocity and ambient oxygen level; it also leads to the

63

inference that smolder velocities tend to be low because of the typically large diffusion length for the oxygen (i.e., because of the slow rate of oxygen supply). Furthermore, on the hypothesis that kinetically-controlled smolder is unstable (and thus will extinguish spontaneously), Williams poses an approximate criterion for smolder extinction: smolder will cease as soon as the kinetic rate of oxygen consumption falls below the diffusive supply rate, i.e., as soon as kinetics become the rate-limiting step in the heat release process. Both hypotheses are qualitatively reasonable but their application to any specific problem will modify and complicate them considerably.

Gugan (89) devised a simple model to explain one feature observed with rod-like fuels smoldering in ambient air, i.e., the roughly conical shape of the steady-state reaction zone as seen, for example, in a quiescently smoldering cigarette. He hypothesized that at the reaction surface, oxygen consumption by reaction is balanced by radial diffusion of oxygen from the surrounding air. Longitudinal diffusion is ignored even though the aspect ratio of the cone is typically near unity. Insertion of a measured smolder velocity into the resulting expression for the reaction surface shape yields a result that is qualitatively like the measured profile. Palmer (11) used a similar idea to explain his observation of depth-dependent upward smolder velocity in deep dust piles. Ohlemiller (24) has used this idea to suggest that the general shape of the reaction zone in Fig. 1 is dominated by oxygen diffusion.

It was noted previously that reverse smolder yields a deflagration wave analogous to a pre-mixed laminar flame. This suggests the application of an

approximate steady-state laminar flame speed theory to this type of problem. Corlett and Brandenburg (38) have applied the Zeldovich/Frank-Kamenetskii/ Semenov (90) theory to reverse combustion in the context of coal gasification. Their approach ignores any considerations about events in the fuel particle interiors, implicitly assuming Zone I behavior (total kinetic control). There appear to be some inconsistencies in the development, incorporation of water and fuel volatilization heats in one part of the analysis while ignoring them in others; the only reaction that is really included is a one-stage exothermic oxidation. The results are qualitatively plausible. The wave speed depends directly on the thermal conductivity of the fuel bed and the rate of heat release. The peak temperature is shown to increase slowly with air supply. The inferred wave thickness is of the order a few centimeters. All of these inferences are in accord with either more detailed smolder models (91) or smolder experiments (18). Corlett and Brandenburg also applied a similar analysis to forward combustion in coal; this is a much more dubious exercise in view of the generally unsteady character of forward smolder.

Numerical Models. Moussa, Toong and Garris (92) did a series of measurements on low density fibrous cellulose cylinders smoldering horizontally in stagnant atmospheres of varying oxygen content. By varying the oxygen percentage and total pressure, they defined a domain of steady, sustained smolder bordered by extinguishment or flaming. The material was basically similar to rope or string. This is a small scale, radially symmetric analog of the smolder situation shown in Fig. 1. As such, it will have a mixed forward/reverse character. Baker's experimental results for cigarette smolder confirm this (25, 26, 27). The smolder configuration is similar to that of

Kinbara, et al, discussed above; it is also quite analogous to the quiescently smoldering cigarette examined by Gugan. The smolder behavior is two-dimensional in character but is treated by a one-dimensional model. The smolder reaction wave is split into two parts for subsequent analysis; a planar interface is assumed to separate an endothermic pyrolysis zone from a char oxidation zone. In view of the later studies of cellulosic materials in Refs. 24 and 28, this concept of a purely endothermic pyrolysis zone is probably incorrect; the high permeability of the cellulose cylinders would readily permit sufficient oxygen to make the region of pyrolysis exothermic (competing oxidative and pyrolytic reactions as discussed in the Smolder Chemistry section). The cellulose pyrolysis is treated in much the same way as is done by Bradbury et al (62), i.e., two competing reactions form either volatiles or a char. The amount of char formed to serve as the sole fuel in the model is then variable, depending on the balance of these two reactions (function of heating rate) but this point is not explored. Since this pyrolysis process is taken to be endothermic, it requires a balancing heat input from the char oxidation zone to permit steady smolder propagation. The char oxidation zone and the pyrolysis zone are coupled together at the hypothetical interface by the heat balancing (and temperature matching) requirement.

The pyrolysis zone is analyzed in some detail; somewhat simplified steady-state analogs of Eq. (13), (15) and the sum of Eq. (16) plus Eq. (20) were solved numerically to infer the requisite input heat flux for a given value of steady smolder velocity. The energy equation is the sum of the two given here because gas and solid are assumed to be in local thermal equilibrium (quite plausible for this problem). The implicit assumption of

66

negligible temperature gradients within the fibrous fuel particles is probably quite good here; internal species gradients do not enter this part of the problem. Exterior surface heat losses are ignored in the pyrolysis region.

The treatment of the char oxidation region is much less detailed and much more approximate. The char oxidation zone is assumed to be an isothermal cylinder of length equal to the cellulose cylinder diameter; oxidation is taken to occur on the outside of this cylinder only. Baker's results (26, 27) for a similar problem, i.e., cigarette smolder, imply that these assumptions are qualitatively plausible but not semi-quantitatively accurate. The char oxidation rate can be limited kinetically (single step reaction) or by mass transfer through a natural convection boundary layer on the exterior of the cellulose cylinder. Heat is lost from the char both by convection and by radiation. The net flux available is dependent on the assumed char temperature (taken equal to the interface temperature); a steady-state model solution occurs where the heat flux (and temperature) matches that demanded by the endothermic pyrolysis zone.

The treatment of the char oxidation zone and the use of a char oxidation expression from the literature (rather than one measured for the particular material) make this a qualitative model. The assumption that the pyrolysis zone of cellulose is endothermic rather than exothermic in this configuration makes the model an even more approximate description of the experimental situation though this assumption may be appropriate for other fuels. The sometimes quantitative agreement between model and experiment shown in the paper must be viewed as fortuitous. As a qualitative description of this type of smolder situation the model appears useful. It predicts that extinguish-

ment occurs with decreasing oxygen availability (ambient oxygen mole fraction) at about the point where the oxidation kinetics are becoming limiting (in rough agreement with William's criterion). It also predicts an increasing smolder velocity and peak smolder temperature with increasing oxygen availability. The model cannot predict the transition from smolder to flaming since it makes no provision for flaming reactions.

Ortiz-Molina (93) and Ortiz-Molina, Toong, Moussa and Tesoro (4) also applied the above model to subsequent studies of smolder propagation in blocks of polyurethane and in composites consisting of polyurethane blocks wrapped with cellulosic materials. The smolder configuration was qualitatively similar to that used above though the samples were bigger in lateral dimensions. The model is as qualitatively applicable to a single foam block as it is to the cellulose cylinders discussed above and again it correlates with some of the experimental trends. Its qualitative applicability to the composite situation is more dubious. Such composites are frequently at the heart of upholstery and bedding smolder but the controlling factors in their smolder have not been adequately studied. The cellulosic outer material can usually smolder on its own; the polyurethane core may or may not smolder on its own. The smoldering behavior of the composite would appear to involve some potentially complex interactions rather difficult to model in any detail. Ortiz-Molina, et al., suggest that the cellulosic fabric merely provides extra heat to sustain the foam core smolder process. While it undoubtedly does do this, further questions such as how the smolder speed and extinguishment limit of the composite are determined remain to be answered.

Muramatsu, Umemura and Okada have, in effect, taken the pyrolysis zone of the same smolder problem as above and treated it in somewhat greater detail; the context is quiescent smolder of a cigarette (64). The model is one-dimensional; Baker's data show that this is a good approximation for this portion of a cigarette (28). The pyrolysis zone is again taken to be non-oxidative; Baker's data (28) make this questionable. Ultimately the tobacco pyrolysis process is taken to be thermoneutral but the heat effect at 0 to 4% oxygen appears most pertinent (28); this has not been determined. Since oxidation is not considered, species gradients in the tobacco particles are not considered. Temperature gradients in the particles are also not considered; for quiescent smolder these are very likely negligible. Steady-state analogs of Eq. (13), (15), (19) and the sum of Eq. (16) plus Eq. (20) are solved numerically. The summation of energy equations is again used because of the assumed local thermal equilibrium between gas and solid. Unlike the analysis of Moussa, et al. above, the energy equation here includes lateral exterior surface losses by convection and conduction; it also includes radiative transfer via a temperature-dependent thermal conductivity. Radiative transfer can become important in low bulk density fuel beds if the radiation path length is a significant fraction (> few %) of the thermal wave thickness. Changes in void fraction (Eq. (10)) are ignored; this is reasonable for this portion of this smolder problem. Water is one of the species leaving the condensed phase. Eq. (19) is applied to water vapor only; a loss term through the permeable paper around the cigarette is included. The rate of water evaporation is described by an empirical expression with an Arrhenius temperature dependence and a power law dependence on the departure of condensed phase water content from a temperature-dependent equilibrium value.

69

The tobacco pyrolysis is taken to occur as a result of four parallel, indepen-
dent reactions gasifying four separate, pre-existing components
(unidentified); the kinetic parameters are measured experimentally. A
measured value of smolder velocity is imposed. The temperature (up to 500°C
and total density profiles show good agreement with measured values. Beyond
500°C the experimental temperature profile bends downward unlike the predicted
profile; this may be due to neglected exothermicity. A somewhat startling
feature of the predicted evaporation of water is that continues all the way up
to a solid phase temperature of 200°C; this has not been checked directly by
experiment. Unfortunately, the limited parametric studies of this model shed
little light on the general problem of factors controlling smolder
propagation.

Quite recently, Leisch (94) modeled the two-dimensional problem shown in
Fig. 1, i.e., smolder propagation in a permeable horizontal fuel layer. The
model, however, is one-dimensional. It considers only steady-state propaga-
tion. The materials of application are grain particle layers (corn/soybean)
and wood sawdust, for which experimental results are also presented. The
model is more general than the previous two above in that pyrolysis and char
oxidation reactions are both allowed everywhere in accord with the Arrhenius
kinetics each follows. Reactions within the grain or wood particles are not
considered, rather they are explicitly assumed to occur only on the outside of
the particles; no justification is given for this. The small particles used
in the experiments are more likely to exhibit Zone I rather than the assumed
Zone III behavior. The reaction kinetic constants for the wood case are
inferred from the literature rather than being measured; for the grain case,
they are backed out of the model predictions after insertion of a measured
smolder velocity.

The model consists of steady-state analogs of Eqns. (13), (15) and the sum of Eq. (16) plus Eq. (20) (without radiative transfer). Again here the use of a single local temperature for gas plus solid is quite justifiable. The one-dimensional energy equation also contains a term describing radiative losses from the top of the fuel layer. A serious deficiency is the failure to include an analog of Eq. (19) for oxygen in spite of the fact that oxygen supply was recognized to be the major controlling factor in the experiments on smolder propagation. Instead, an assumed "average" level of oxygen is used in the char oxidation kinetic expressions. As a result, the model becomes completely kinetically-controlled in its heat release rate rather than oxygen supply rate-controlled. The few computed values of smolder velocity are in reasonably good agreement with experiment but this is not a particularly meaningful test since the average oxygen level is, in effect, a floating parameter; the value used, 0.16 atm, is seen to be quite high when reference is made to Fig. 1.

Cigarette smolder during the in-draw of air is a forward propagation problem, albeit a specialized one. Summerfield, Ohlemiller and Sandusky (45) developed a one-dimensional unsteady model of this process during a constant draw (steady flow) from ignition. The real problem is very much two-dimensional on the smolder wave scale and may even have significant species gradients in the tobacco particles (it appears to be a borderline case). The two-dimensionality on the smolder wave scale is due to the tendency of the peripheral cigarette paper to burn back allowing air to preferentially enter the cigarette at the base of the coal (21, 95); this causes the peripheral region to burn much faster than that near the tobacco rod centerline (21). The question of species gradients in the particles does not seem to have been

explored in the context of this problem; the present author is not aware of any pore size distribution data for tobacco. The results of Baker (35) imply that this question is pertinent to oxidation only below 400°C; above this temperature, external mass transfer is found to control the rate of oxidation of the solid. In the model of Summerfield, et al., the 2-D effects due to paper burn-back are approximated in a 1-D manner; the air inflow resistance of the paper is assumed to drop to a very small value when the temperature of the adjacent tobacco is greater than a fixed paper burn temperature. Gradients within the particles are assumed negligible throughout the entire smolder zone. Only two reactions were included: non-oxidative pyrolysis and char oxidation; kinetic expressions were obtained at the much lower heating rates found in thermal analysis. Water behavior was not included; for this fuel, water could play a significant role in modifying temperature profiles. Endothermic char gasification by CO_2 was not included though Baker shows it to be significant in real cigarettes (35). Unsteady versions of Eq. (13), (15), (16), (17)-(20) were solved for the special conditions of high gas flow rate such that smolder wave-scale species diffusion and heat conduction are small compared to convection (small π_{9j} and π_{11}). Radiative transfer in the solid is included by means of the forward/reverse approximation. Note that the local gas and solid temperatures are not assumed to be equal; Baker's data for cigarettes show differences of more than 100°C in some regions even at a low flow rate (2 cm^3/s) (25).

The model was not extensively tested although it does correctly predict the upward trend of smolder velocity with oxidizing gas flow rate and oxygen content. In agreement with Baker, the char oxidation process is found to be limited by external mass transfer. The good quantitative agreement with

72

experiment in the paper is mostly a fortuitous result of the choice of paper burn-back temperature. The predicted smolder velocity is very sensitive to this parameter because it controls the amount of inflowing air that bypasses the hottest part of the char oxidation zone. This same phenomenon makes these model results a rather poor basis for interpreting other forward smolder situations. For example, because of this air bypass route, this forward smolder problem does not have the oxygen profile structure shown in Fig. 3 for a 1-D reaction wave and its qualitative behavior is not constrained in the same ways as were discussed in conjunction with that figure. In particular, there is no longer a very simple relation between total rate of oxygen inflow and the rate of movement of the char oxidation zone. Some of the noted parameter effects are probably qualitatively applicable to other, more typical forward smolder problems in some circumstances. An increase in the convective heat transfer coefficient between bulk gas and bulk solid caused a nearly proportional increase in smolder wave speed; this should apply only to the pyrolysis portion of a wave such as that in Fig. 3 and only when convective heat transfer dominates over conduction/radiation. Suppression of radiative transfer in a few test cases of this problem caused a large increase in peak reaction zone temperature; evidently it constitutes a substantial mechanism for heat dissipation from this zone. Order of magnitude changes in the preexponential kinetic factors for the two overall reactions had minimal effect on the problem; this is indicative of oxygen-supply-rate-limited behavior.

The most detailed model of reverse smolder propagation presently in the literature is that of Ohlemiller, Bellan and Rogers (91). This is a 1-D, time-dependent model based on analogs of Eq. (13), (14), (16), (17) to (20). Gas and solid energy equations are combined on the assumption of local thermal

73

equilibrium; local species equilibrium between gas and solid is also assumed (large π_{2K}, π_{12}, π_{22K}, π_{29}, π_{30K}). Wave-scale diffusion is included. Radiative transfer is included by means of the forward/reverse approximation. The model is applied to smolder propagation in a polyurethane foam where the initial characteristic particle dimension was 0.1 to 1 mm. Particle scale gradients were not explicitly considered in this paper. Subsequently it was reported that the pores in the char are mainly in the 20-80 Å range. The char dimensions and time scales studied were such that temperature and oxygen gradients in the charred particles were thus quite small. However the initial foam material had no pore structure so that oxidative attack on the initial fuel particles was undoubtedly diffusion limited; gas diffusivities in the solid phase tend to be several orders of magnitude less than those in even the smallest pores. This was not explicitly modeled. Instead the kinetic parameters for the only two reactions included in the model were obtained by thermal analysis using samples with the same foam structure. Because of the differences in heating rates (5X or more) this is bound to be somewhat inaccurate, but it is difficult to estimate how much so. Water behavior is not included; polyurethanes contain minimal moisture but may form it during smolder.

The model solutions correctly predict the qualitative trends of behavior seen with the polyurethane foam, i.e., increasing smolder velocity and peak temperature with increased O_2 supply and the differing rates of increase depending on how O_2 supply is increased (higher velocity with fixed O_2 level or fixed velocity with increasing O_2 level). Quantitatively the model is less successful, predicting temperatures and smolder velocities that are somewhat low. It is inferred that, like virtually every other smolder propagation

74

process, this reverse smolder process is oxygen-supply-rate-limited (as opposed to kinetically limited). The rate of propagation is set by a balance between the rate of heat generation (proportional to the rate of oxygen supply) and the rate of heat transfer (conduction plus radiation) to the next element of fuel. Reaction kinetics in this model serve only to dictate the distribution of the oxygen between the two reaction pathways included. Cutting the pre-exponential factor of the dominant char oxidation reaction by 10X had no effect on the total rate of heat generation (all O_2 continued to be consumed in a thicker wave) and it produced only a small decrease in propagation rate.

Reverse smolder tends to leave part of the char behind as a residue since the wave typically engulfs (heats and "ignites") the next element of fuel before the first element is all consumed. This residue is an insulator against the only path for heat losses in such one-dimensional propagation, i.e., losses from the originally ignited end of the fuel bed. This model shows that this insulating residue plays a significant role in helping the fuel bed achieve a self-sustaining smolder situation. If the reaction kinetics are slowed thus making ignition more difficult, sustained heating will eventually build up a residue layer that will insulate the slowed reaction and allow it to sustain and propagate itself. It is unclear whether the model thus implies ignition can always be achieved no matter how slow the reaction kinetics (the limit would seem to be adiabatic ignition). Such a prediction is overly pessimistic with regard to the real world where 2-D heat losses would impose a lower limit on kinetic rates able to support self-sustained smolder propagation. Nevertheless there is a strong implication that large decreases in kinetic rates must be achieved by smolder retardants

to suppress reverse smolder. Because of its very limited chemical description, this model misses another pathway to smolder suppression, i.e., fuel pyrolysis. This process is endothermic, typically, and it removes material that could be oxidized heterogeneously to sustain smolder. Exploration of this would require only a slight extension of the model. This model was not capable of predictions about transition to flaming since it included no gas phase reactions.

Models in Related Problem Areas. It was noted previously that there are several other combustion problems that qualitatively resemble smolder propagation. The problem area that has received the most analysis is gasification of coal and oil shale both in situ and in packed bed reactors. Both forward and reverse propagation are employed; reverse propagation may be used to establish a high permeability channel for subsequent use in a forward propagation mode. Numerous models, of varying degree of approximation, have been developed to explain the parametric dependence of propagation velocity and to predict the evolved gas composition (37, 96-108). The chemistry involved is rather different from smoldering as are various parameter values affecting propagation; in addition, the fuel bed permeabilities may be much lower implying strong pressure gradients. Nevertheless, the gross qualitative behavior should pertain to smoldering under some conditions. Here we briefly examine the nature and results of a few of the most complete models.

The forward propagation models in Refs. 104, 105 and 106 are all basically the same. These are one-dimensional models based on analogs of Eq. (10) (with $v_p = 0$), (13), (15), (16) and Eq. (17)-(20). Diffusion in the bulk gas phase is neglected with minimal justification; it appears to be

potentially significant for at least some cases considered. It is recognized that there probably are particle-scale gradients in part (or all) of the range of coal or oil shale particles encountered in practice. However, the role of these gradients is essentially ignored at this modeling stage. Heterogeneous reactions are either in Zone I or Zone III. The number of reactions considered is large, e.g., eleven in Ref. 106. The reason for this is the attempt to predict the major effluent species and hence the heating value of the gas. Both gas phase and heterogeneous oxidation are included but the former is treated in a manner that obscures its real significance. These models are reasonably successful in predicting the rate of movement of the reaction and condensation fronts as well as the major gas constituent levels for the few cases compared with experiment. They appear to comprise the best qualitative description of 1-D forward "smolder" propagation currently in the literature. The temperature profile is qualitatively the same as that in Fig. 3; the predicted dependence of propagation velocity on oxygen input level is qualitatively the same as that found experimentally in Ref. 18 for smolder propagation through a bed of wood fibers. Unfortunately these models have not been exercised in a way which sheds much further light on the forward smolder propagation problem.

Reverse combustion of coal and oil shale appears to have received rather less modeling effort. The model of Kotowski and Gunn (37) is fairly detailed though substantially less so than the forward models just discussed. This is a steady-state, 1-D model based on analogs of Eq. (17), (19) and (20); the energy equation is for the combined gas plus solid since the two temperatures are assumed locally equal. Diffusion is again neglected even though it may be important for some cases studied. Particle-scale gradients are not

considered. A conservation equation for the condensed phase fuel is avoided by a heuristic description of the temperature-dependent fraction of volatilized material. (This sort of empiricism misses the heating-rate-dependent temperature shift in the gasification process.) Only one reaction appears in the energy equation, gas phase oxidation of fuel vapors. Water vaporization is considered as a heat sink but not as a rate process. The resulting temperature and oxygen profiles resemble those in Fig. 3. Propagation velocity and peak reaction wave temperature increase with oxygen supply in agreement with experiment. Increased fuel bed conductivity is predicted to increase the propagation velocity as expected. An unexpected (and unexplained) prediction is that an increased pre-exponential rate factor will decrease the propagation velocity; this is contrary to the expectation based on the simple deflagration model of Corlett and Brandenburg (38) mentioned above. The model of Amr (108) is time-dependent and slightly more detailed than that of Kotowski and Gunn but basically similar; the limited parametric studies do not add further insights pertinent to smolder propagation.

There have been some linear stability analyses of forward and reverse propagation in the context of in situ gasification. In this gasification process, one attempts to propagate a reaction wave between drill holes into the fuel seam below ground. It is of interest to determine what parameters determine whether the reaction front will be broad and flat or will contract into channels. The reverse combustion stability analysis of Gunn and Krantz (109) is based on perturbations of a very rough steady-state propagation model (gas/solid energy equation with conduction and convection only; final temperature an imposed function of gas velocity). The solutions predict that reverse propagation is unstable at low gas velocities, particularly toward large

wavelength disturbances. The results are used by the authors to explain several anomalous experimental aspects of reverse combustion in coal seam tests as being due to channeling (diameter about 1 meter). Krantz, Keyashian, Zollars and Gunn (110) also did a linear stability analysis based on the same type of steady-state propagation model for wet forward (and reverse) propagation. Wet in this case implies sufficient water for the steam vaporization and the combustion fronts to coincide. In view of Fig. 3, this type of model seems to be an even rougher approximation for forward propagation. The solutions predict that forward wet combustion is unstable for many conditions of interest to _in situ_ gasification. Experimentally, less water-saturated forward combustion in coal seams is found to be stable.

Most recently Britten and Krantz (112) did a linear stability analysis of a more complex reverse propagation model. Analogs of the sum of Eqns. (13) plus (17), the sum of Eq. (16) plus Eq. (20) and Eq. (19) for gas phase oxygen were solved analytically by asymptotic expansion. Radiative transfer was not included. Neglect of wave-scale diffusion in the gas phase oxygen equation was justified by restriction of the solution domain to very large Lewis numbers pertinent to very low porosity coal seams. Only one reaction was considered, gas phase oxidation of fuel vapors arising from the condensed phase; the gasification of these vapors was not explicitly included in the model equations. (A related model by Britten and Krantz (113), analyzed similarly, considers only direct heterogeneous oxidation of the solid.)

The zeroth order solutions (steady-state) are basically similar to the phenomenological model of Corlett and Brandenburg (38). The predicted variations of peak temperature and propagation velocity with flow rate of the

oxidizing gas are quite reasonable. The zeroth and first order solutions were spatially perturbed about a planar front to determine which wave numbers of spatial disturbance grow. The model predicts a stable planar front only in the absence of a change in permeability of the solid across the reaction zone. For all other cases, there is a disturbance wavelength (whose value depends on the various parameters) which is amplified more rapidly than any other. The results are shown to be plausibly in accord with the limited data on the behavior of in situ coal burns.

In contrast to these stability predictions for in situ gasification, the present author has found, in small scale laboratory tests (15-25 cm diameter fuel beds), forward smolder propagation readily goes unstable even at very low flow velocities (few mm/s) while reverse smolder is stable at least to 1 cm/s gas flow velocity. Egerton, Gugan and Weinberg (21) reported that continued forward smolder in cigarettes is highly unstable. These results do not necessarily contradict each other given the small scale of the smolder experiments, the 2-D influence of a peripheral boundary not accounted for in the preceding analyses and the large disparity in parameter values in the two types of experiments, particulary fuel bed permeability.

Concluding Remarks

The general problem of smoldering combustion propagation in particulate fuel beds is very complex both chemically and thermophysically. Since the starting material is a polymer or mix of polymers, the number of elementary reactions involved becomes indefinitely large posing a problem much more complex than the well-studied, related problem of carbon oxidation. It is not

80

feasible to model all of these reactions even if they are someday elucidated for even one common smolder-prone substance such as cellulose. The engineering approach around this problem has been the use of a few overall lumped "reactions" with apparent kinetic parameters determined typically by thermal analysis. The potential pitfalls here due to disparities in heating rate have not been adequately explored. It must be borne in mind that this engineering approach to the chemistry can only help quantify the relative role of chemistry in the total problem. It cannot provide any real insights about chemical solutions to the problem of smolder propagation.

The thermophysical problem can be more explicitly described but the complexity of the resulting equations precludes, general solutions. The general case is made intractable by the existence of species and temperature gradients simultaneously on the fuel particle scale and on the reaction wave scale. Given this, one must start with simplified cases in an effort to build a body of knowledge about the quantitative interactions among the numerous model parameters. The current state of development is quite inadequate. Even the 1-D limiting cases of forward and reverse smolder with no particle-scale gradients are not fully characterized. The qualitative nature of their behavior is reasonably well understood. The dominant role of oxygen supply rate is recognized.

The seemingly secondary role of oxidation kinetics during self-sustained propagation is deceptive. Any realistic solution to smolder propagation in smolder-prone materials such as cellulosics will almost certainly be chemical in nature. Most product uses preclude physical approaches such as inhibiting oxygen supply rate and, in any event, smolder has a propensity to adapt

tenaciously to even very low oxygen supply rates. The role of kinetics enters
in setting the level of the ignition temperature (or heat flux) and the condi-
tions for extinguishment. Some qualitative models such as that of Moussa,
Toong and Garris nicely demonstrate the principles involved but require
considerable elaboration in order to be fully realistic. The limiting cases
of 1-D forward and reverse smolder are not particularly useful in this regard;
they are unusually resistant to extinguishment because of their 1-D character
and they approximate relatively few real world smolder problems. A fully
developed model of the problem in Fig. 1 would provide the first basis for
quantitative exploration of all the chemical and physical factors involved in
sustained smolder of a realistic configuration.

Finally, it should be pointed out that the opposite boundary on smolder
behavior, transition to flaming, has only been superficially explored experi-
mentally and not modeled at all. The process is implicit in the general model
equations above given the right boundary conditions, but the nature of the
phenomenon is only dimly understood. Since transition from smolder to flaming
poses a sudden increase in life hazard, much more effort is needed toward
understanding and controlling this process.

References

1. Clarke, F. and Ottoson, J., *Fire J.*, May 1976, p. 20.

2. McCarter, R., *J. Consumer Prod. Flamm.* **3**, 128 (1976).

3. Rogers, F., Ohlemiller, T., Kurtz, A. and Summerfield, M. *J. Fire Flamm.* **9**, 5 (1978).

4. Ortiz-Molina, M, Toong, T.-Y., Moussa, N. Tesoro, G., *Seventeenth Symposium (International) on Combustion*, The Combustion Institute, Pittsburgh (1978) p. 1191.

5. Drysdale, D., *Fire Prev. Sci. Technol.* **23**, 18 (1980).

6. Quintiere, J., Birky, M., McDonald, F. and Smith, G., "An Analysis of Smoldering Fires in Closed Compartments and Their Hazard Due to Carbon Monoxide", National Bureau of Standards, NBSIR 82-2556, July 1982.

7. Zicherman, J. and Fisher, F., "Fire Protection Problems Associated With Cellulose Based Insulation Products", Society of Fire Protection Engineers Technology Report 78-7 (1978).

8. Gross, D., "A Preliminary Study of the Fire Safety of Thermal Insulation for Use in Attics or Enclosed Spaces in Residential Housing, National Bureau of Standards, NBSIR 78-1497 (1978).

9. Ohlemiller, T. and Rogers, F., *Combust. Sci. Technol.* **24** 139 (1980).

10. Ohlemiller, T. *Combust. Sci. Technol.* **26**, 89 (1981).

11. Palmer, K. *Combust. Flame I*, 129 (1957).

12. McCarter, R., *J. Fire Flamm.* **9**, 119 (1978).

13. Ohlemiller, T. and Rogers, F., "Smoldering Combustion Studies of Rigid Cellular Plastics", Princeton University Mechanical and Aerospace Engineering Report No. 1432, May 1979.

14. Anon., "Self-Heating of Organic Materials, (Proceedings of an International Symposium) Delft, Holland, 1971.

15. Kayser, E. and Boyars, C., "Spontaneously Combustible Solids-A Literature Study", Naval Surface Weapons Center Report NSWC/WOL/TR-75-159 (1975).

16. Palmer, K. *Dust Explosions and Fires*, Chapman and Hall, London, 1973.

17. Leisch, S. Kaufman, C. and Nicholls, J., "Smoldering Combustion as Related to Grain Elevator Safety", University of Michigan Dept. of Aerospace Engineering Report UM-388164-F, June 1982.

18. Ohlemiller, T. and Lucca, D., "An Experimental Comparison of Forward and Reverse Smolder Propagation in Permeable Fuel Beds", Combustion and Flame, 54, 131 (1983).

19. Cohen, L. and Luft., Fuel 34, 154 (1955).

20. Kinbara, T. Endo, H. and Sega, S., Eleventh Symposium (International) on Combustion, The Combustion Institute, Pittsburgh, Pa. (1967) p. 525.

21. Egerton, A. Gugan, K. and Weinberg, F., Combust. Flame 7, 63 (1963).

22. Gann, R., Earl., W., Manka, M. and Miles, L., Eighteenth Symposium (International) on Combustion, The Combustion Institute, Pittsburgh, Pa. (1980) p. 571.

23. Rogers, F. and Ohlemiller, T., J. Fire Flamm. 11, 32 (1980).

24. Ohlemiller, T., "Smoldering Combustion Hazards of Thermal Insulation Materials" National Bureau of Standards NBSIR-81-2350 (1981).

25. Baker, R., Nature 247, No. 5440, 405 (1974).

26. Baker, R. and Kilburn, K., Beitrage Zur Tabakforschung, 7, 79 (1973).

27. Baker, R. Combust. Flame 30, 21 (1977).

28. Baker, R., Beitrage Zur Tabakforschung International 11, 1 (1981).

29. Gray, P. and Lee, P., "Thermal Explosion Theory" in Oxidation and Combustion Reviews (C.F. Tipper, ed), Vol. 2, Elsevier, New York (1967).

30. Thomas, P., "Self Heating and Thermal Ignition-A Guide to Its Theory and Application" in Ignition, Heat Release and Noncombustibility of Materials", ASTM STP-502, Philadelphia, Pa. (1972).

31. Day, M. and Wiles, D., J. Consumer Prod. Flamm. 5, 113 (1978).

32. McCarter, R., Fire and Materials 5, 66 (1981).

33. De Soete, G., Eleventh Symposium (International) on Combustion, The Combustion Institute, Pittsburgh, Pa. (1967) p. 959.

34. Lewis, B. and Von Elbe, G., Combustion, Flames and Explosions of Gases (2nd ed.), Academic Press, New York (1961) p. 124.

35. Baker, R., Thermochimica Acta 17, 29 (1976).

36. Dryer, F., "High Temperature Oxidation of Carbon Monoxide and Methane in a Turbulent Flow Reactor", Princeton University Aerospace and Mechanical Sciences Dept. Report T-1034 (1972).

37. Kotowski, M. and Gunn, R., "Theoretical Aspects of Reverse Combustion in the Underground Gasification of Coal", USDOE Laramie Energy Research Center Report LERC/RI-76/4, Laramie, Wyoming (1976).

38. Corlett, R. and Brandenburg, C. "Combustion Processes in In Situ Coal Gasification: Phenomena, Conceptual Models and Research Status. Part I - Overview and Continuum Wave Descriptions", Western States Section/Combustion Institute Paper WSS/CI 77-3 (1977).

39. Cullis, C. and Hirschler, M., The Combustion of Organic Polymers, Clarendon Press, Oxford (1981).

40. Benbow, A. and Cullis, C., "The Mechanism of Ignition of Organic Compounds and Its Catalysis by Inorganic Materials" paper presented at Joint Central States, Western States Section/Combustion Institute Meeting, April 1975.

41. Shafizadeh, F., Bradbury, A., DeGroot, W. and Aanerud, T., I & EC Prod. Res. Devel. 21, 97 (1982).

42. Ohlemiller, T. J., results to be published.

43. Shafizadeh, F. and Sekiguchi, Y., Combust. Flame 55, 171 (1984).

44. Rogers, F. and Ohlemiller, T., Combust. Sci. Technol., 24, 129 (1980).

45. Summerfield, M., Ohlemiller, T. and Sandusky, H., Combust.Flame 33, 263 (1979).

46. Muramatsu, M. and Umemura, S., Beitrage Zur Tabakforschung 11, 79 (1981).

47. Shafizadeh, F. and Bradbury, A., J. Appl. Poly. Sci. 23, 143 (1979).

48. Bradbury, A. and Shafizadeh, F., Carbon 18, 109 (1980).

49. Shafizadeh, F. and Sekiguchi, Y., Carbon 21, 511 (1983).

50. Sekiguchi, Y., Frye, J. and Shafizadeh, F., J. Appl. Poly. Sci. 28, 3513 (1983).

51. Gan, H., Nandi, S. and Walker, P., Fuel 51, 272 (1972).

52. Laurendeau, N., Prog. Energy Combust. Sci. 4, 221 (1978).

53. Simons, G. and Finson, M., Combust. Sci. Technol. 19, 217 (1979).

54. Simons, G., Combust. Sci. Technol. 19, 227 (1979).

55. Shafizadeh, F. and Bradbury, A., J. Thermal Insul. 2, 141 (1979).

56. Bradbury, A. and Shafizadeh, F., Combust. Flame 37, 85 (1980).

57. McCarter, R., J. Consumer Prod. Flamm. 4, 346 (1977).

58. Shafizadeh, F. Bradbury, A. and De Groot, W., "Formation and Reactivity of Cellulosic Chars" paper presented at Western States Section/ Combustion Institute (1981).

59. McKee, D., "The Catalyzed Gasification Reactions of Carbon" in The Chemistry and Physics of Carbon, (P. Walker and P. Thrower, eds.) Marcel Dekker, New York (1981).

60. Gregg, D. and Olness, D. "Basic Principles of Underground Coal Gasification", Lawrence Livermore Laboratory, Preprint UCRL-52107, August 1976.

61. Jellinek, H. (ed.), Aspects of Degradation and Stabilization of Polymers, Elsevier, New York (1978).

62. Bradbury, A., Sakai, Y. and Shafizadeh, F., J. Appl. Poly. Sci. 23, 3271 (1979).

63. Perry, J. (ed.), Chemical Engineers Handbook, 3rd ed. McGraw-Hill, New York (1950), p. 800-808.

64. Muramatsu, M. Umemura, S. and Okada, T., Combust. Flame 36, 245 (1979).

65. Baker, R., Prog. Energy Combust. Sci. 7, 135 (1981).

66. Hedges, J. "Ignition and Pyrolysis of Polymer Films", Ph. D. Thesis, Univ. of Utah, Dept. of Chem. Eng., June 1978.

67. Anthony, D. Howard, J., Hottel, H. and Meissner, H. Fifteenth Symposium (International) on Combustion, The Combustion Institute, Pittsburgh, Pa. (1974), p. 1303.

68. Flynn, J. and Wall, L., J. Res. Nat'l Bur. Stds. Sect. A 70, 487 (1966).

69. Jellinek, H. (ed.) ibid, chap. 12.

70. Rogers, F. and Ohlemiller, T., J. Macromol. Sci-Chem. A15(1), 169 (1981).

71. Lewis, B. and Von Elbe, G., ibid, Chap III.

72. Walker, P., Rusinko, F. and Austin, L., "Gas Reactions of Carbon" in Advances in Catalysis XI, 133 (1959).

73. Szekely J., Evans, J. and Sohn, H., Gas-Solid Reactions, Academic Press, New York (1976).

74. Szekely, J., Evans, J. and Sohn, H., ibid, p. 109-111.

75. Szekely, J. Evans, J. and Sohn, H. ibid, chap. 7.

76. Szekely, J. Evans, J. and Sohn, H., ibid, p. 30.

77. Hottel, H. and Sarofim, A., Radiative Transfer, McGraw Hill, New York (1967) pp. 430-433.

78. Stanek, V. and Szekely, J., Canad. J. Chem Eng. 50, 9 (1972).

79. Hellums, J. and Churchill, S., Chem. Eng. Prog. Sympos. Series, No. 32 Vol 57, 75 (1961).

80. Szekely, J., Evans, J. and Sohn, H., ibid, p. 263.

81. Szekely, J. Evans, J. and Sohn, H., ibid, p. 152.

82. Smith, J., Chemical Engineering Kinetics 2nd ed, McGraw-Hill, New York (1970), p. 446.

83. Bird, R., Stewart, W. and Lightfoot, E, Transport Phenomena, Wiley, New York (1960), p. 198.

84. DeRis, J., Combust. Sci. Technol. 2, 239 (1970).

85. Johnson, B., Froment, G. and Watson, C., Chem. Eng. Sci. 17, 835 (1962).

86. Sega, S., Bull. Jap. Assoc. Fire Sci. Eng. 25, 17 (1975).

87. Sega, S., Bull. Jap. Assoc. Fire Sci. Eng. 25, 25 (1975).

88. Williams, F., Sixteenth Symposium (International) on Combustion, The Combustion Institute, Pittsburgh, Pa. (1976) p. 1281.

89. Gugan, K., Combust. Flame 10, 161 (1966).

90. Glassman, J., Combustion, Academic Press, New York (1977) p. 68-75.

91. Ohlemiller, T., Bellan, J. and Rogers, F., Combust. Flame, 36, 197 (1979).

92. Moussa, N., Toong, T.-Y., and Garris, C., Sixteenth Symposium (International) on Combustion, The Combustion Institute, Pittsburgh, Pa. (1976) p. 1447.

93. Ortiz-Molina, M., Ph.D Thesis, Dept. of Mechanical Engineering, Massachusetts Institute of Technology, June 1980.

94. Leisch, S., "Smoldering Combustion in Horizontal Dust Layers", Ph.D. Thesis, University of Michigan Aerospace Engineering Dept., November 1983.

95. Baker, R., Nature, 264, No. 5582, 167 (1976).

96. Mayers, M., Trans. ASME 59, No. 4, 279 (1937).

97. Silver, R., Fuel, XXXII, 121 (1953).

98. Koizumi, M., Sixth Symposium (International) on Combustion, Reinhold, New York (1956) p. 577.

99. Gottfried, B., Soc. Petrol-Eng. J., Sept. 1965, p. 196.

100. Gottfried, B., Combust. Flame, Feb. 1968, p. 5.

101. Gunn, R. and Whitman, D., "An In Situ Coal Gasification Model (Forward Mode) For Feasibility Studies and Design", DOE Laramie Energy Research Center Rept. LERC/RI-76/2, Laramie, Wyoming (1976).

102. George, J. and Harris, H., Siam J. Numer. Anal. 14, 137 (1977).

103. Dockter, L. and Harris, H., "A Mathematical Model of Forward Combustion Retorting of Oil Shale", DOE Laramie Energy Technology Center Rept. LETC/TPR-78/1, Laramie, Wyoming, 1978.

104. Winslow, A., Sixteenth Symposium (International) on Combustion, The Combustion Institute, Pittsburgh, Pa., (1976) p. 503.

105. Thorsness, C. and Rozsa, R., "Lawrence Livermore Laboratory In Situ Coal Gasification Program: Model Calculations and Laboratory Experiments", Lawrence Livermore Laboratory Preprint UCRL-78302, Livermore, Ca., (1976).

106. Thorsness, C., Grens, E. and Sherwood, A., "A One-Dimensional Model For in Situ Coal Gasification Lawrence Livermore Laboratory Rept. UCRL-52523, (1978).

107. Branch, M., Prog. Energy Combust. Sci. 5, 193 (1979).

108. Amr, A., Combust. Flame 41, 301 (1981).

109. Gunn, R. and Krantz, W., Society of Petroleum Engineers Paper SPE-6735, Oct. 1977.

110. Krantz, W., Keyashian, M., Zollars, R. and Gunn, R., Society of Petroleum Engineers Paper SPE 7523, Oct. 1978.

111. Smith, J., ibid, p. 365.

112. Britten, J. and Krantz, W., "Linear Stability of Planar Reverse Combustion in Porous Media", presented at 1984 Spring Meeting, Western States Section, Combustion Institute, Boulder, Colorado.

113. Britten, J. and Krantz, W., Proc. NATO Workshop on Chemical Instabilities, Austin, Texas, March 1983.

Nomenclature

a_{PD} - empirical constant relating drag on gas flowing through fuel particle pores to gas flow velocity.

$A_{VP\ell}$ - surface area/unit volume of particle available for reaction; this factor drops out of rate expressions for volumetric reactions such as pyrolysis.

$\bar{C}_{PO}$ - specific heat of initial (unburned) fuel particles.

c_1, c_2 - coefficients for laminar and turbulent drag terms, respectively in differential Ergun equation.

A_{VB} - external fuel particle area/unit volume of fuel particle bed.

g_x - component of gravitational acceleration in x direction.

D_{eb} - effective diffusivity or dispersion coefficient for gas species in bulk gas of fuel particle bed.

D_{ep} - effective diffusivity of gases in particle pores.

E - activation energy.

H - heat transfer coefficient for flow around exterior of fuel particle.

89

h_{GP} - sensible enthalpy per unit mass of gas in fuel particle

        pores $\equiv \Sigma_j \left(Y_{jGP} h_{jGP.} \right)$

h_{jGP} - sensible enthalphy per unit mass of gaseous species j in fuel

        particle pores.

h_P - sensible enthalpy per unit mass of solid in fuel

        particle $\equiv \Sigma_j \left(Y_{jP} \, h_{jP.} \right)$

K - mass transfer coefficient for flow around exterior of fuel

        particle.

ℓ_R - reference length in non-dimensionalization.

n_{ox} - overall stoichiometry of smolder wave, mass of oxygen/unit mass of

        fuel consumed.

n_P - number of particles/unit volume of fuel particle bed.

P - local pressure of gas in bulk gas around fuel particle.

P_P - pressure of gas in particle pores.

P' - local pressure deviation from hydrostatic value.

Q_{EXO} - net exothermicity of smolder wave per unit mass of fuel consumed.

$Q_{\ell,STP}$ — heat of reaction ℓ per unit mass of reactant, measured at standard temperature and pressure.

$Q_{\ell,T}$ — heat of reaction ℓ per unit mass of reactant, measured at local reaction temperature.

$Q_{m,STP}$ — heat of reaction m per unit mass of reactant, measured at standard temperature and pressure.

R — universal gas constant.

R_{mj} — rate of reaction of bulk gas species j/unit volume of fuel bed.

$R_{P\ell}$ — rate of reaction ℓ in fuel particle; (mass/unit volume) or (mass/unit area).

r — dimension perpendicular to particle surface (radius, half-thickness); a = 0 for slab-like particles; a = 1 for cylindrical particles; a = 2 for spherical particles.

t — time.

S — net radiation flux vector due to solid fuel particle emission/absorption/scattering.

T_A — effective ambient temperature for buoyancy force.

91

T_G — local temperature of bulk gas around fuel particles.

T_P — local temperature of solid in fuel particle.

v_{GP} — velocity of gas in fuel particle pores.

v_{Gx}, v_{Gy} — components of bulk gas velocity in X and Y directions; also denoted v_x, v_y in Eq. (22).

$V_B(m/m_o)$ — bulk volume of fuel particle bed (gas + solid) assumed dependent only on fraction of initial solid mass that remains, (m/m_o).

Y_{jG} — local mass fraction of gas species j in bulk gas around fuel particles.

Y_{jGP} — local mass fraction of gaseous species j in fuel particle pores.

Y_{jP} — local mass fraction of solid species j in fuel particle.

z — pre-exponential factor in chemical reaction rates.

$\dot{\Lambda}_P$ — rate of change of flow displacement volume of a fuel particle.

λ_E — thermal conductivity of bulk fuel particle bed (gas + solid).

λ_P — thermal conductivity of fuel particle.

92

$\nu_{F\ell j}$ - stoichiometric coefficient (mass basis) for formation of gaseous species j from reaction ℓ in fuel particle.

$\nu_{C\ell j}$ - as above but for consumption of j.

$\nu_{G\ell}$ - mass of gas produced per unit mass of solid reactant consumed.

μ_{GF} - viscosity of gas in particle pores.

ϕ - porosity (fractional free volume) of fuel particle bed.

ϕ_P - porosity (fractional free volume) within a fuel particle.

ρ_{BO} - initial bulk density of fuel particle bed.

ρ_{GF} - density of gas within a fuel particle.

ρ_P - density of solid part of fuel particle.

$\sum_{KP}$ - summation over all gaseous species in pores of fuel particles.

$\sum_{\ell}$ - summation over ℓ reactions occurring in fuel particle.

$\sum_{m}$ - summation over m reactions involving gas species in bulk gas phase.

93

$\sum\limits_{KG}$ - summation over all the gaseous species present in bulk gas (and in

particle pores).

Subscripts

A   - ambient

0   - initial value

R   - reference value

Table I

EXPERIMENTAL CHARACTERISTICS OF SMOLDER PROPAGATION

Ref. No.	Fuel	Fuel/Smolder Geometry	Air Supply condition/rate	Smolder Velocity, $\frac{cm}{sec}$	Maximum Temp. (°C)	Comment
19	coal dust (>104µ)	1 cm thick horiz. layer/ lateral spread	natural convection/ diffusion	$1.7 \cdot 10^{-3}$	460	bulk density not given
19	sawdust (75-150µ)	1 cm thick horiz. layer/ lateral spread	natural convection/ diffusion	$4.0 \cdot 10^{-3}$	(170)*	smol. vel. increased with layer depth; *(temp. dubious)
11	cork dust (<65µ) (0.18 g/cc)	1.65 cm thick horiz. layer/ lateral spread, forward smolder	flow over top of layer/50-700 $\frac{cm}{sec}$	$7 \cdot 10^{-3}-1.8 \cdot 10^{-2}$	790 at 200 $\frac{cm}{sec}$ 840 at 600 $\frac{cm}{sec}$	smol. vel. increased monotonically w. air vel.
11	cork dust (<65µ) (0.18 g/cc)	1.65 cm thick horiz. layer/ lateral spread, reverse smolder	flow over top of layer/75-800 $\frac{cm}{sec}$	$5 \cdot 10^{-3}-6 \cdot 10^{-3}$	not given	smol. vel. independent of air vel. above 400 cm/sec
11	vegetable fiber board (0.27 g/cc)	1.3 cm thick board/ upward spread	natural convec./diffus.	$4.5 \cdot 10^{-3}$	not given	smol. vel. 2X less if board is horizontal
20	rolled paper	0.4-0.8 cm diam. cylin./ downward spread	natural convec./diffus.	$5.0-8.4 \cdot 10^{-3}$	not given	smol. vel. increased with decreasing diam.
21	tobacco shreds	cigarette, 0.8 cm diam.	Intermittent nat'l convec./diffus., and forced draw 30 $\frac{cm}{sec}$ through tob rod	$4.5 \cdot 10^{-3}$ (nat'l convec.) <.15 (periphery during draw)	850°C (nat'l convec.) <1200°C (draw)	highly transient behavior
22	cellulose fabric +3% NaCl	double fabric layer 0.2 cm thick/horiz. spread, weakly forward smol.	flow over exterior, 10 $\frac{cm}{sec}$	$1.0 \cdot 10^{-2}$	770	smol. vel., temp. dependent on additives
23	flexible polyurethane foam (.04 g/cc)	nearly 1-D/reverse smolder	uniform flow through foam/0.15-0.45 $\frac{cm}{sec}$	$1.0-1.8 \cdot 10^{-2}$	430-475	smol. vel. and temp. increased w. gas flow vel. and with increasing % O_2
25	cellulostic loose-fill insulation (wood fibers) (.04 g/cc)	1-D/reverse smolder	uniform through fiber bed/0.04-0.75 $\frac{cm}{sec}$	$4.5 \cdot 10^{-3}$ to $3.7 \cdot 10^{-2}$	430-640	smol. vel., temp. increased monotonically w. air flow
25	cellulostic loose-fill insulation (wood fibers) (.04 g/cc)	approx. 1-D/forward smolder	uniform through fiber bed/0.15-0.48 $\frac{cm}{sec}$	1.0 to $2.5 \cdot 10^{-3}$	535-595	smol. vel. temp. increased monotonically w. air flow

95

Table II
Dimensionless Groups with Approximate Magnitudes

<u>Definitions of reference quantities and estimated ranges for key values:</u>

$$T_R = \left(Q_{EXO} / \bar{C}_{po} \right)$$
625 – 1500 K

$$V_{GR} = \left(\frac{\phi_o g_x \rho_A}{c_1 \mu_R} \right) \left(\frac{T_R - T_A}{T_R} \right)$$
$10^{-4} - 10^{-1}$ m/s

$$V_{PR} = \left(\frac{V_{GR} \rho_{GO} Y_{oxo}}{n_{ox} \rho_{BO}} \right)$$
$10^{-7} - 10^{-3}$ m/s

$$\ell_R = \left(\frac{T_R \lambda_{BO}}{\rho_{BO} V_{PR} C_{PO} (T_R - T_o)} \right)$$
$10^{-3} - 1$ m

$$t_R = \ell_R / V_{PR}$$
$1 - 10^4$ s

$$V_{GPR} = \left((1-\phi) \rho_P V_{PR} / \rho_{GPR} A_{VBR} \ell_R \right)$$

$$P_R = \left(C_1 \mu_R V_{GR} \ell_R / \phi_R \right)$$

$$P_{PR} = \left(r_{PR} c_{1R} \mu_{GPR} V_{GPR} / \phi_{PR} \right)$$

h_{GR}, h_{PR}, etc. (all enthalpy ref. values) = $\bar{C}_{po} (T_R - T_o)$

Y_{KGR}, Y_{KGPR}, Y_{KPR} = initial or maximum values

ϕ, ϕ_R, λ_{BR}, λ_{PR}, ρ_{GR}, ρ_{PR}, ρ_{GPR} = initial or maximum values

$\dot{V}_R$, S_R, A_{VBR}, $A_{VP\ell R}$, D_{epR}, D_{eBR} = maximum values

96

Dimensionless groups and magnitudes employing above quantities:

$$\pi_1 = \left(\ell_R / t_R V_{GR}\right) \qquad\qquad O(10^{-3})$$

$$\pi_{2K} = \left(KA_{VBR} \ell_R Y_{KGPR} / V_{GR} \rho_{GR} \phi_R\right) \qquad\qquad O(10^{-2} - 10^3)$$

$$\pi_3 = \left(\phi_R \rho_{GR} / t_R c_1 \mu_R\right) \qquad\qquad O(10^{-2} - 10^{-9})$$

$$\pi_4 = \left(\phi_R \rho_{GR} V_{GR} / \ell_R c_1 \mu_R\right) \qquad\qquad O(10^{-3} - 1)$$

$$\pi_5 = \left(\phi_R g_x \rho_A / c_1 \mu_R V_{GR}\right) \qquad\qquad O(1)$$

$$\pi_6 = \left(c_2 V_{GR} / c_1 \mu_R\right) \qquad\qquad O(10^{-6} - 10)$$

$$\pi_{7K} = \left(KA_{VBR} Y_{KGPR} / c_1 \mu_R\right) \qquad\qquad O(10^{-4} - 1)$$

$$\pi_{8j} = \left(\ell_R Y_{jGR} / t_R V_{GR}\right) \qquad\qquad O(10^{-3})$$

$$\pi_{9j} = \left(D_{eBR} Y_{jGR} / \ell_R V_{GR}\right) \qquad\qquad O(.1 - 1)$$

$$\pi_{10mj} = \left(\ell_R (\nu_F - \nu_C)_{mj} Z_m \left(\rho_{GR} Y_{OXR}\right)^{a_m} \left(\rho_{GR} Y_{GFMR}\right)^{b_m} \exp\left(-E_m / RT_{GR}\right) / \rho_{GR} V_{GR}\right) \qquad O(1)$$

$$\pi_{11} = \left(T_R \lambda_{ER} / \ell_R \rho_{GR} V_{GR} h_{GR}\right) \qquad\qquad O(.1 - 1)$$

$$\pi_{12} = \left(hA_{VBR} T_R \ell_R / \rho_{GR} \phi_R Y_{GR} h_{GR}\right) \qquad\qquad O(10^{-2} - 10^4)$$

$$\pi_{13mj} = \pi_{10mj} \left(Q_{m,STP} / h_{GR} \left(\nu_F - \nu_C \right)_{mj} \right) \qquad 0(1)$$

$$\pi_{14} = \left(\ell_R \phi_R / V_{PR} t_R \right) \qquad 0(1)$$

$$\pi_{15} = \phi_R \qquad 0(.1 - 1)$$

$$\pi_{16} = \phi_{PR} \qquad 0(.1 - 1)$$

$$\pi_{17} = \left(n_p \dot{\Lambda}_{PR} \ell_R / V_{PR} \right) \qquad \leq 0(1)$$

$$\pi_{18\ell} = \left(\nu_{G\ell} A_{VP\ell R} Z_{P\ell} \left(\rho_{GPR} Y_{OXPR} \right)^{a_{P\ell}} \left(\rho_{PR} Y_{P\ell R} \right)^{b_{\ell}} \exp \left(-E_{P\ell} / RT_R \right) \ell_R / V_{PR} \rho_{PR} \right) \qquad 0(1)$$
$$\equiv \left(RR_{\ell} \ell_R / V_{PR} \rho_{PR} \right)$$

$$\pi_{19} = \left(\rho_{GPR} \phi_{PR} / t_R RR_1 \right) \qquad 0(10^{-3})$$

$$\pi_{20} = \left(\phi_{PR} V_{PR} \rho_{GPR} / \ell_R RR_1 \right) \qquad 0(10^{-3})$$

$$\pi_{21\ell} = \left(RR_{\ell} / RR_1 \right) \qquad \leq 0(1)$$

$$\pi_{22K} = \left(K A_{VBR} Y_{KGPR} / RR_1 \right) \qquad 0(10^{-4} - 10^4)$$

$$\pi_{23j} = \left(\phi_{PR} \rho_{GPR} Y_{jGPR} / t_R RR_1 \right) \qquad 0(10^{-3})$$

$$\pi_{24j} = \left(\phi_{PR} \rho_{GPR} V_{PR} Y_{jGPR} / \ell_R RR_1 \right) \qquad 0(10^{-3})$$

$$\pi_{25\ell j} = \left(\left(\nu_F - \nu_c \right)_{\ell j} / \nu_{G\ell} \right) \qquad 0(1)$$

98

$$\pi_{26j} = Y_{jGPR} \qquad\qquad 0(1)$$

$$\pi_{27} = \left(\phi_{PR}\rho_{GPR}h_{GPR}/\rho_{PR}h_{PR}\right) \qquad\qquad 0(10^{-3})$$

$$\pi_{28} = \left(S_R/\rho_{PR}V_{PR}h_{PR}\right) \qquad\qquad \leq 0(1)$$

$$\pi_{29} = \left(HA_{VBR}T_R\ell_R/\rho_{PR}V_{PR}h_{PR}\right) \qquad\qquad 0(10^{-2} - 10^4)$$

$$\pi_{30K} = \left(KA_{VBR}Y_{KGPR}h_{GPR}\ell_R/\rho_{PR}V_{PR}h_{PR}\right) \qquad\qquad 0(10^{-4} - 10^4)$$

$$\pi_{31\ell} = \left(Q_{\ell,STP}/\nu_{G\ell}h_{PR}\right) \qquad\qquad 0(1)$$

$$\pi_{32} = \left(\rho_{GPR}/t_R RR_1\right) \qquad\qquad 0(10^{-3})$$

$$\pi_{33} = \left(\rho_{GPR}V_{GPR}/r_{PR}RR_1\right) \qquad\qquad 0(1)$$

$$\pi_{34} = \left(\rho_{PR}/t_R RR_1\right) \qquad\qquad 0(1)$$

$$\pi_{35} = \left(\rho_{GPR}V_{GPR}r_{PR}/P_{PR}t_R\right) \qquad\qquad 0(10^{-15} - 10^{-3})$$

$$\pi_{36} = \left(\rho_{GPR}V_{GPR}^2/P_{PR}\right) \qquad\qquad 0(10^{-10} - 1)$$

$$\pi_{37\ell} = \left(r_{PR}V_{GPR}RR_\ell/P_{PR}\right) \qquad\qquad 0(10^{-10} - 1)$$

$$\pi_{38j} = \left(\rho_{PR}Y_{jPR}/t_R RR_1\right) \qquad\qquad 0(1)$$

$$\pi_{39j} = \left(\phi_{PR}\rho_{GPR}Y_{jGPR}/t_R RR_1\right) \qquad\qquad 0(10^{-3})$$

$$\pi_{40j} = \left(\rho_{GPR}\phi_{PR}V_{GPR}Y_{jGPR}/r_{PR}RR_1\right) \qquad\qquad \leq 0(1)$$

$$\pi_{41j} = \left(\rho_{GPR}D_{ePR}Y_{jGPR}/r_{PR}^2 RR_1\right) \qquad\qquad 0(10^{-6} - 10^4)$$

$$\pi_{42} = \left(\rho_{GPR}\phi_{PR}D_{ePR}/r_{PR}K\right) \qquad\qquad 0(10^{-6} - 1)$$

$$\pi_{43\ell j} = \left(\phi_{PR}RR_\ell/A_{VP\ell R}KY_{jPGR}\right) \qquad\qquad 0(10^{-4} - 1)$$

$$\pi_{44} = \left(\rho_{PR}h_{PR}\nu_{G1}/t_R Q_{1,STP}RR_1\right) \qquad\qquad 0(0.1 - 1)$$

$$\pi_{45} = \left(\phi_{PR}\rho_{GPR}h_{GPR}\nu_{G1}/t_R Q_{1,STP}RR_1\right) \qquad\qquad 0(10^{-4} - 10^{-3})$$

$$\pi_{46} = \left(\phi_{PR}\rho_{GPR}V_{GPR}h_{GPR}\nu_{G1}/\nu_{PR}Q_{1,STP}RR_1\right) \qquad\qquad \leq 0 \ (0.1 - 1.0)$$

$$\pi_{47} = \left(\lambda_{PR}T_R\nu_{G1}/r_{PR}^2 Q_{1,STP}RR_1\right) \qquad\qquad 0(10^{-3} - 10^4)$$

$$\pi_{48K} = \left(h_{KGPR}\rho_{GPR}D_{ePR}Y_{KGPR}\nu_{G1}/r_{PR}^2 Q_{1,STP}RR_1\right) \qquad\qquad 0(10^{-6} - 10^4)$$

$$\pi_{49} = \left(h_{PR}\nu_{G1}/Q_{1,STP}\right) \qquad\qquad 0.(0.1 - 1.0)$$

$$\pi_{50\ell} = \left(Q_{\ell,STP}RR_\ell/Q_{1,STP}RR_1\right) \qquad\qquad \leq 0(1)$$

$$\pi_{51\ell} = \left(h_{PR}\nu_{G\ell}/Q_{\ell,STP}\right) \qquad\qquad 0(0.1 - 1)$$

$$\pi_{52} = \left(\lambda_{PR}/r_{PR}H\right) \qquad\qquad 0(0.1 - 100)$$

$$\pi_{53\ell} = \left(Q_{\ell,STP}\phi_{PR}RR_{\ell}/\nu_{G\ell}A_{VP\ell R}HT_R\right) \qquad\qquad 0(10^{-4} - 10^4)$$

$$\pi_{54} = \left(\phi_{PR}\rho_{GPR}V_{GPR}/K\right) \qquad\qquad \leq 0(1)$$

$$\pi_{55} = \left(\phi_{PR}\rho_{GPR}V_{GPR}h_{GPR}/HT_R\right) \qquad\qquad \leq 0(1)$$
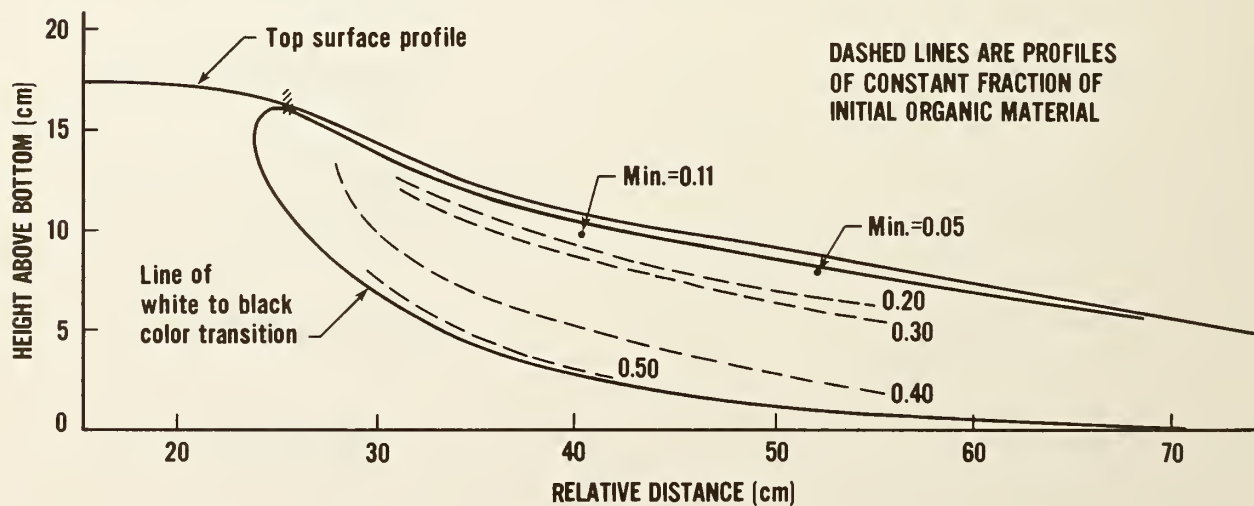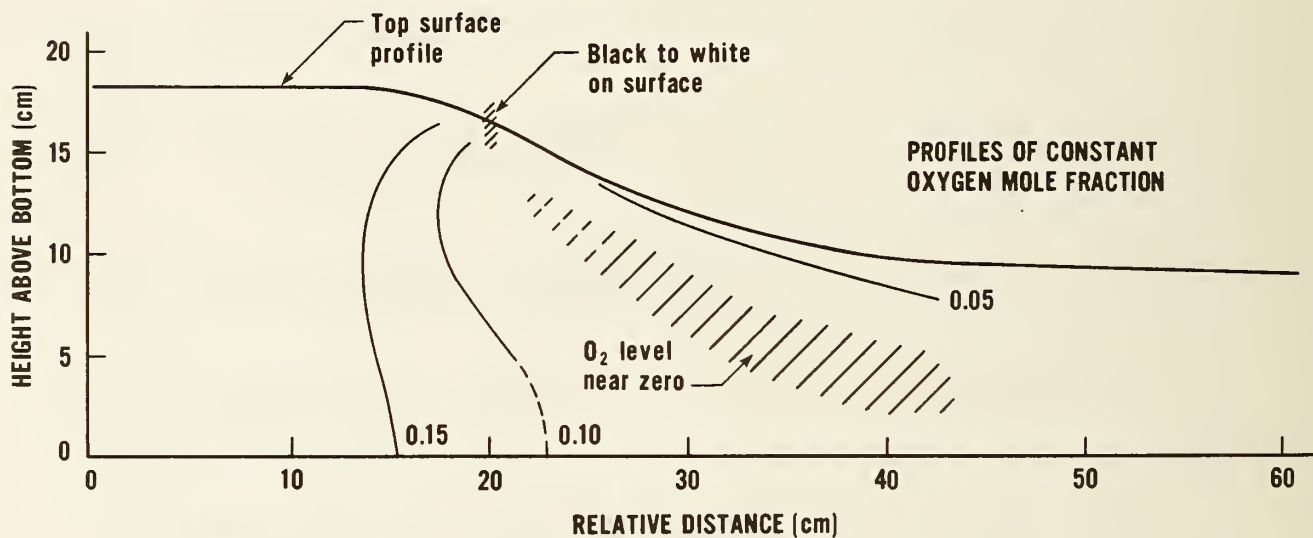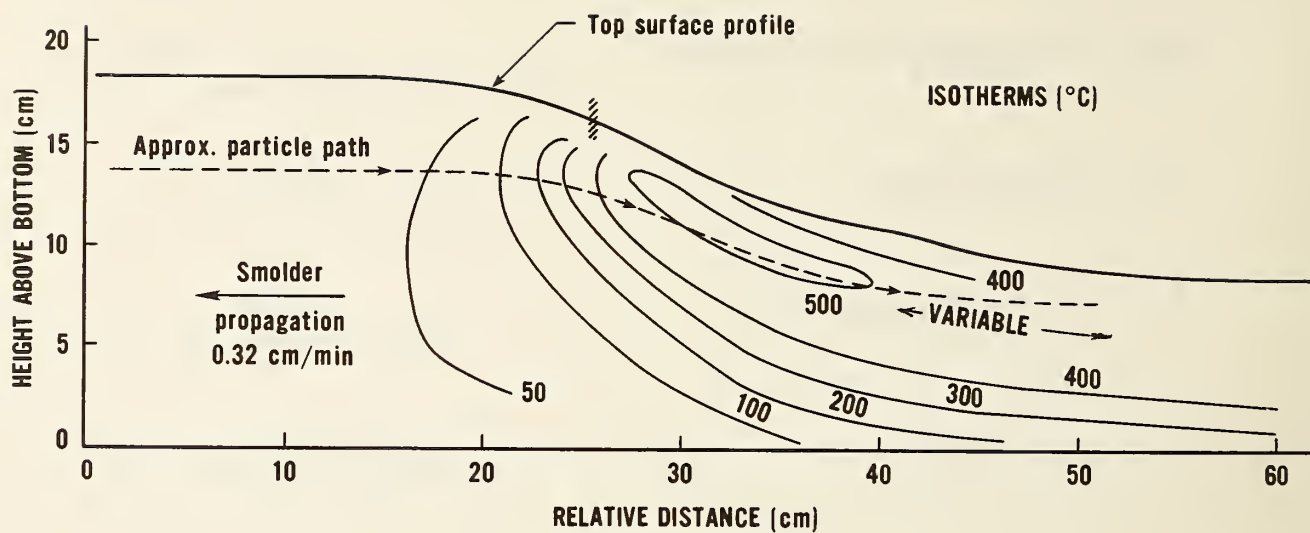
Fig. 1) Example of smolder wave structure in a permeable horizontal fuel layer; wood fibers with bulk density of 0.04 g/cm^3. From ref. 24.
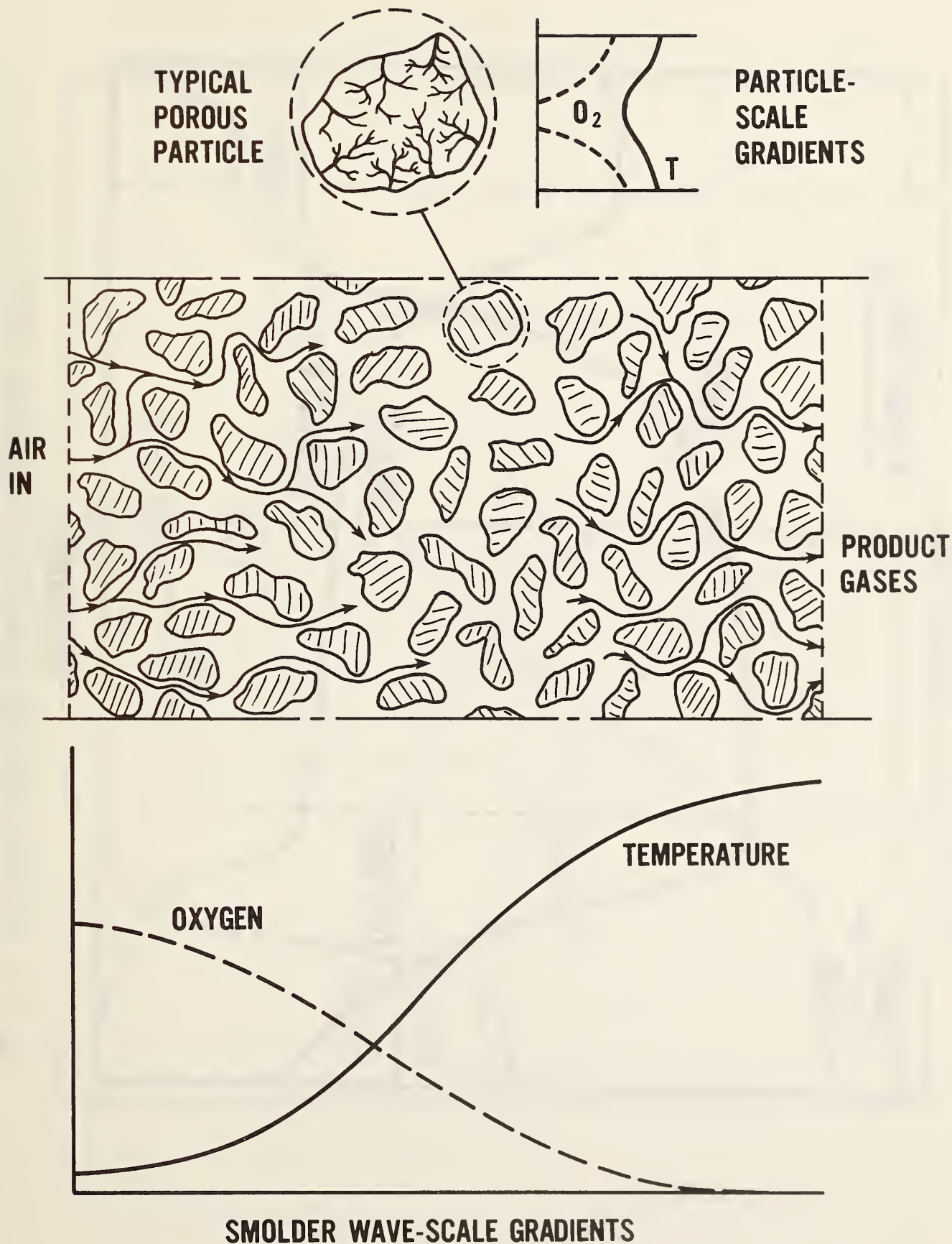
TYPICAL POROUS PARTICLE

PARTICLE-SCALE GRADIENTS

O_2

T

AIR IN

PRODUCT GASES

TEMPERATURE

OXYGEN

SMOLDER WAVE-SCALE GRADIENTS

Fig. 2) General structure of a smolder wave in a bed of fuel particles showing gradients on wave scale and on particle scale.
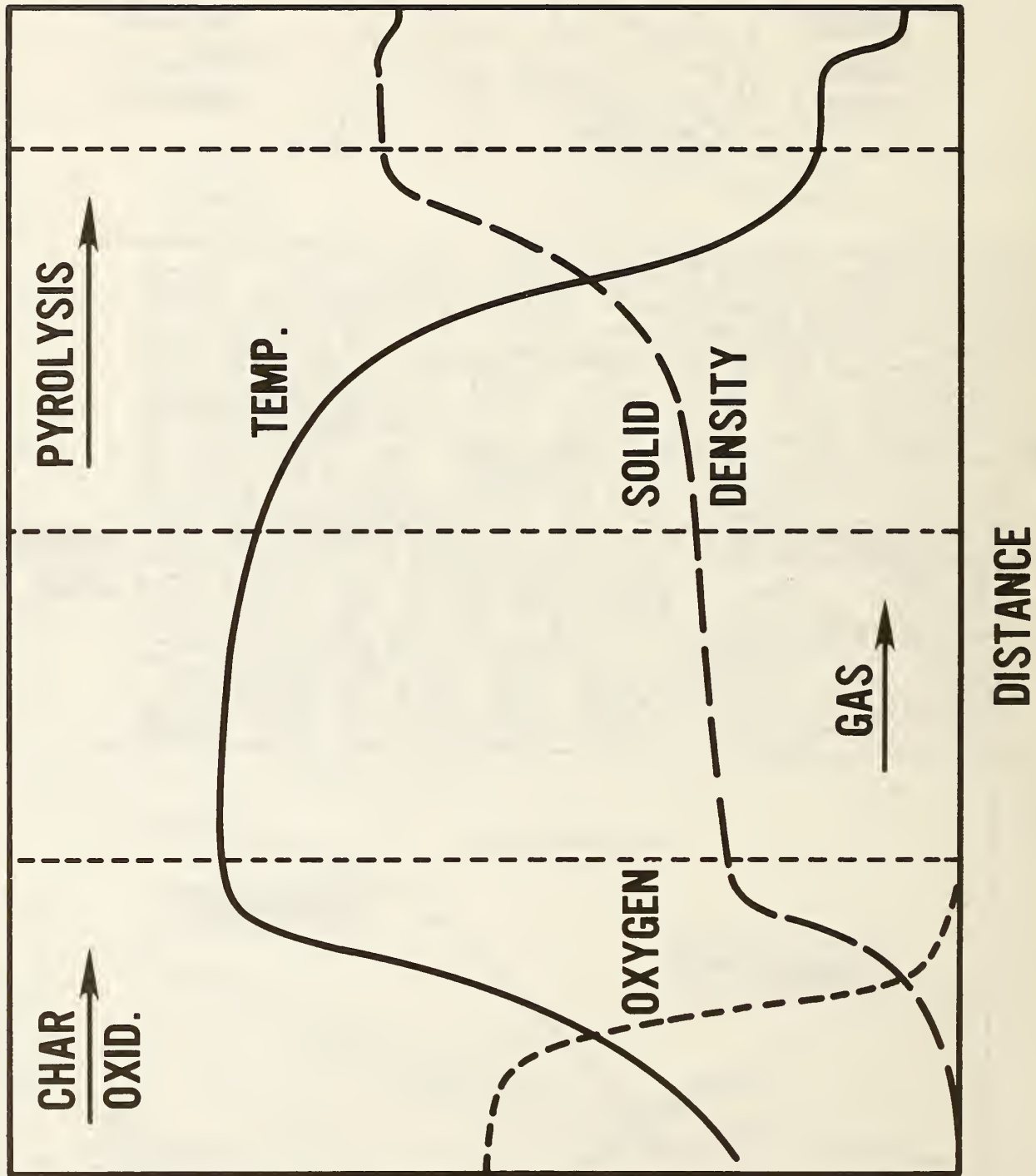
103

Fig. 3(a). Profiles of temperature, oxygen concentration and solid density for typical case of forward smolder (from ref. 18).
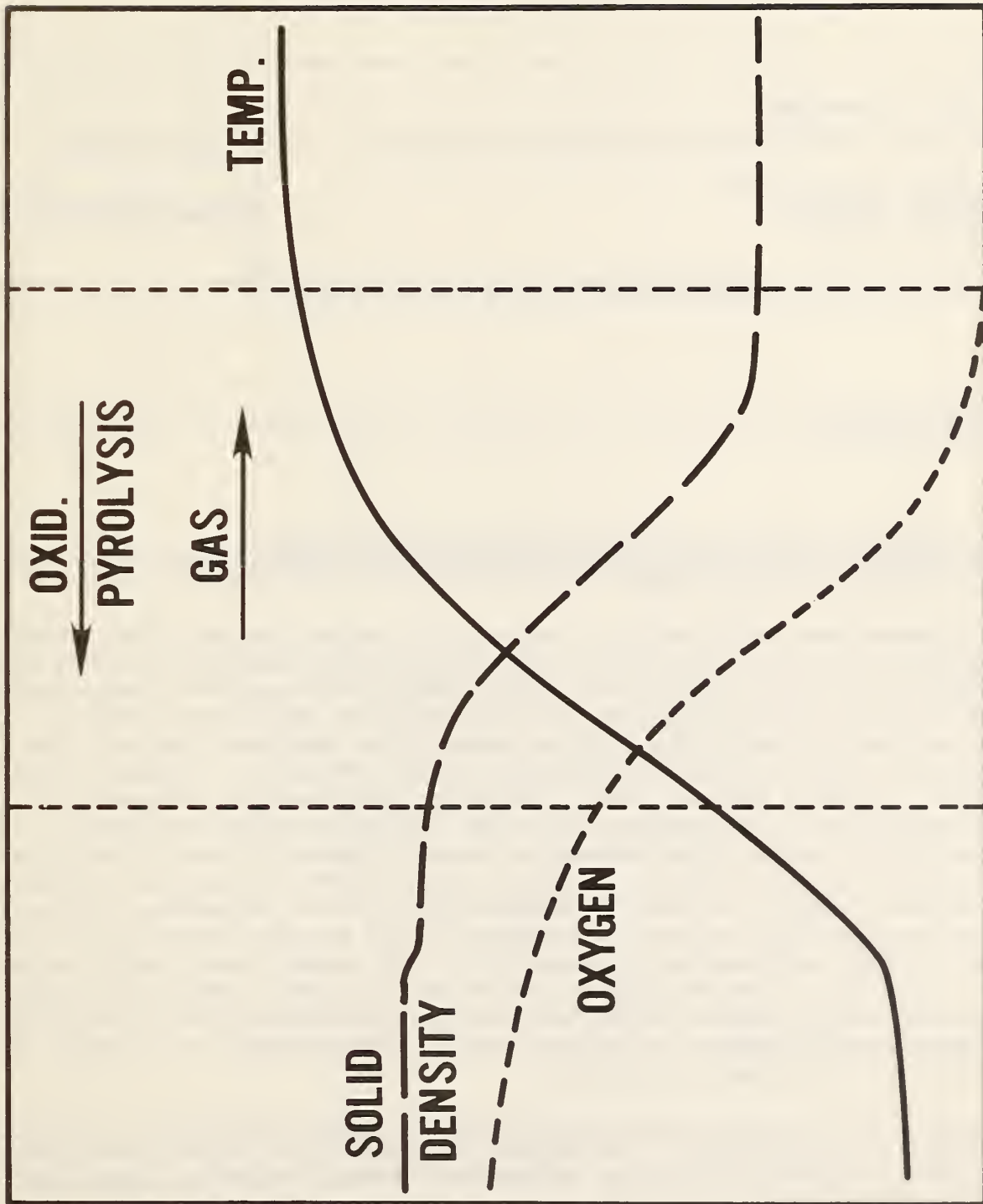
Fig. 3(b). Profiles of temperature, oxygen concentration and solid density for typical case of reverse smolder (from ref. 18).

U.S. DEPT. OF COMM. **BIBLIOGRAPHIC DATA SHEET** (See instructions)	1. PUBLICATION OR REPORT NO. NBSIR 84-2895	2. Performing Organ. Report No.	3. Publication Date June 1984

4. TITLE AND SUBTITLE

Modeling of Smoldering Combustion Propagation

5. AUTHOR(S)

T.J. Ohlemiller

6. PERFORMING ORGANIZATION (If joint or other than NBS, see instructions) **NATIONAL BUREAU OF STANDARDS DEPARTMENT OF COMMERCE WASHINGTON, D.C. 20234**	7. Contract/Grant No.
	8. Type of Report & Period Covered

9. SPONSORING ORGANIZATION NAME AND COMPLETE ADDRESS (Street, City, State, ZIP)

10. SUPPLEMENTARY NOTES

☐ Document describes a computer program; SF-185, FIPS Software Summary, is attached.

11. ABSTRACT (A 200-word or less factual summary of most significant information. If document includes a significant bibliography or literature survey, mention it here)

Smoldering combustion, which can pose a serious life safety hazard, is encountered most frequently in various cellulosic materials and in open-cell polyurethane foams. It is probable that the principal heat source driving this process is heterogeneous oxidation but gas phase reactions may also contribute at higher temperatures. The chemistry involved is best-defined for the case of pure cellulose but even here the details are limited and actual mechanisms poorly understood; simplified kinetic descriptions, typically derived from isothermal or theromoanalytical experiments, currently provide the only tractable inputs for smoldering combustion models. The general problem of smolder wave propagation through a permeable bed of fuel particles is posed; coupled to the chemistry, one must also consider the physical processes of heat and mass transfer on both the particle scale and on the smolder wave scale. The general equations can be somewhat simpified, after non-dimensionalization, for cases where certain dimensionless parameters are very large or very small compared to unity. Existing smolder propagation models are all greatly simplified compared to this general model, neglecting gradients on the particle scale and considering only one-dimensional gradients on the wave scale. These models are reviewed; their contributions and deficiencies are noted.

12. KEY WORDS (Six to twelve entries; alphabetical order; capitalize only proper names; and separate key words by semicolons)

cellulosics; combustion; plastics; polyurethane foams; smoldering combustion

13. AVAILABILITY [X] Unlimited ☐ For Official Distribution. Do Not Release to NTIS ☐ Order From Superintendent of Documents, U.S. Government Printing Office, Washington, D.C. 20402. [X] Order From National Technical Information Service (NTIS), Springfield, VA. 22161	14. NO. OF PRINTED PAGES 111
	15. Price $13.00